JSEE Vol. 26, No. 3, 2024 DOI: 10.48303/jsee.2024.2009752.1074

Technical Note

An Investigation on the Accuracy of Wavelet-Based Down-Sampling in Seismic Structural Analysis

Noorollah Majidi[1*], Alireza Jalili[2] and Ali Heidari[3]

1. Ph.D., Department of Civil Engineering, University of Isfahan, Isfahan, Iran, *Corresponding Author; email: n.majidi@trn.ui.ac.ir
2. M.Sc. Student, Department of Civil Engineering, Khorasgan Branch, Islamic Azad University, Isfahan, Iran
3. Associate Professor, Department of Civil Engineering, Shahrekord University, Shahrekord, Iran

Received: 06/09/2023
Revised: 06/07/2024
Accepted: 14/07/2024

Keywords:
Wavelet transform;
Wavelet function;
Computational costs;
Nonlinear analysis;
Dynamic analysis;
Down-sampling method

ABSTRACT

Wavelet transforms have been used for 20 years to reduce dynamic analysis costs, with studies suggesting the use of this method for three levels of decomposition. In addition, in these studies, the time step of the solution is assumed to be equal to the time step of the earthquake record and therefore the stability of the numerical method is essential in such cases. Also, in previous studies, the effects of the distance from the fault on the accuracy of the approximate waves have not been evaluated. This paper examines the accuracy of wavelet-based down-sampling methods for 50 far-field, near-field, and pulse-like earthquake records and 24 wavelet functions. Also, two numerical methods, Newmark's average acceleration and the interpolation-based method are studied. The results of this research show that Newmark's average acceleration method is suitable for wavelet-based dynamic analysis. Also, in this study, it is shown that by choosing the appropriate wavelet function, even up to four levels of decomposition may be used with an error of less than 2%. Therefore, with this work, the cost of calculations may be reduced up to 16 times.

How to cite the article:
Majidi, N., Jalili, A., & Heidari, A. (2024). An Investigation on the Accuracy of Wavelet-Based Down-Sampling in Seismic Structural Analysis. Journal of Seismology and Earthquake Engineering, 26(3), 63-87. doi: 10.48303/jsee.2024.2009752.1074

1. Introduction

In dynamic analysis, if the time step of the input load is smaller than the accuracy time step of the numerical solution method, it can lead to an increase in the cost of calculations (Majidi et al., 2023). Therefore, the use of down-sampling methods can help increase the time step of dynamic loads. In the dynamic analysis of structures with dominant mode period of more than 2 seconds under earthquake load, the time step of the earthquake is often larger than the time step of the accuracy of the numerical method (Soroushian, 2008). Therefore, in this category of analysis, by increasing the time step of the earthquake, the time step of the solution can also be increased. Using wavelet-based down-sampling methods is one of the smart ways to increase the time step of earthquake records (Majidi et al., 2023).

Several down-sampling techniques employ linear and nonlinear interpolations to extend the time step of earthquake recordings. Soroushian (2008) implemented a straightforward interpolation approach to decrease the number of ground motion data points, significantly reducing the computational expenses associated with structural analysis. Subsequent investigations by Nateghi (2011) utilized this method for dynamic analysis of a silo, while Soroushian et al. (2011) applied it to reduce computation costs in reservoir analysis, demonstrating its effectiveness for real-world structures. Hosseini et al. (2013) employed the short-time Fourier transform to streamline computational efforts in analyzing SDOF structures. However, it's important to acknowledge that these methods may introduce calculation errors if they fail to account for the frequency characteristics of earthquake records when increasing time steps. Majidi et al. (2023) showed that if the frequency characteristics of earthquake records are not considered in the process of reducing sampling, the calculation error increases.

The use of wavelet transform to decrease time steps in earthquake records was first investigated on structures with linear behavior (Salajegheh & Heidari, 2002). In another study, Salajegheh and Heidari (2004) used Haar or Daubechies1 wavelet transform and artificial neural networks to reduce computations related to the optimization process of a modified genetic algorithm. In this study, the cross-sectional area of the members of a two-dimensional truss was optimized and the cost of optimization calculations was reduced more than 80% with an error of less than 8%. They also studied the wavelet filter bank method in other research and showed that the cost of calculations was reduced by 90% considering a calculation error about 7% (Salajegheh & Heidari, 2005).

The challenge of high computational cost is more important in the dynamic analysis of non-linear systems, and therefore application of DWT method on these problems should be investigated. Heidari et al. (2019) used discrete wavelet transform to reduce the computational cost of calculating nonlinear response spectra. They studied 20 earthquake records and 6 ductility coefficients and used Daubechies 4 wavelet transform in their research. The maximum error of the estimated response spectra at the third stage of filtering was up to 70% while its average value was 25%. In another study, Kamgar et al. (2020) analyzed a 7-story structure using nonlinear beam column elements of OpenSees software. They used Haar wavelet transform and examined it for 8 far-field and near-field earthquake records. They showed that the approximate waves of the third stage of filtering have an error of less than 5%. Dadkhah et al. (2020) performed incremental dynamic analyses for a two-dimensional 6-story structure with concentrated plastic hinges using Haar wavelet transform. They studied approximate waves of 15 near-fields and far-fields earthquake records. They compared the drift ratios and the base shear of the structure at different intensity measures for the approximate waves and original ones. The average error of these parameters for the approximate waves of the third stage of filtering was between 2% to 13%. Kamgar et al. (2021) reduced the cost of calculations in the dynamic analysis of structures considering the effects of soil-structure interaction. They studied 20, 25, 30 and 35 story structures for 20 different earthquake records. These records were filtered up to 5 stages using the Daubechies4 wavelet transform. The calculation errors of the maximum displacement of the structures for the approximate waves of the third stage of filtering were up to 90%, but in

most cases the errors were between 2 and 36%. Kamgar et al. (2022) examined the performance of the Daubechies4 wavelet function to reduce the cost of IDA. They examined the response of SDOF systems for 12 earthquake records and found the calculation error up to 35% for this wavelet function. In 2021, Javdanian et al. (2021) studied the use of wavelet-based down-sampling methods to obtain site responses. In this study, they evaluated only one soil profile and 42 earthquakes (42 analyses). In this study, only the response of single-degree of freedom systems was investigated. In this paper, the obtained results show the proper performance of wavelet transform in eliminating high frequencies of earthquake waves. In other words, in this article, wavelet transform was used as a mathe-matical tool to remove high frequencies in order to remove noise in the earthquake record.

In 2023, for the first time, Majidi et al. (2023) investigated the effect of wavelet functions on the accuracy of wavelet-based down-sampling methods. In this study, 36 wavelet functions and 100 earthquake records related to soils of different types were analyzed. In this study, earthquake records were decomposed to 3 levels.

Also, the effects of the distance of the earthquake record from the fault, as well as the effect of the numerical method of integration on the accuracy of the calculations, were not evaluated.

By reviewing previous studies, it can be seen that several points have not yet been investigated in wavelet-based down-sampling methods. The first problem is to choose the appropriate wavelet function in order to increase the accuracy of these methods in levels 4 and 5 of decomposition. The reason for the importance of this issue is the significant reduction of calculations at these levels. In other words, in the wavelet method, for each level of decomposition, the cost of calculations can be reduced by 2 times. Therefore, the first to fifth decomposition levels can reduce the calculation cost by 2 times, 4 times, 8 times, 16 times and 32 times, respectively. The next discussion that has been neglected in these studies is the investigation of the effect of numerical integration methods on the accuracy of down-sampling. Also, in these studies, the effects of the distance from the fault on the accuracy of down-sampling methods have not been investigated. In this regard, in the following, 50 earthquake records far from the fault and near the fault are decomposed up to 5 levels using wavelet transformation.

Also, 24 wavelet functions that have been proposed in various studies to reduce the sampling of earthquake records are evaluated. Besides, the performance of two numerical methods of integration is also checked on these approximate waves. In the end, a 20-story steel structure with approximate waves obtained from wavelet transformation will be investigated.

2. Wavelet Transform

Wavelet transform is a tool for frequency analysis of waves (Mallat, 1999). Wavelet transform can extract the time and frequency information of the wave simultaneously by using two characteristics of scale and shift. In wavelet transform, scale involves analyzing signals at different resolutions, capturing broad features at higher scales and finer details at lower scales. Shift refers to moving the analyzing window across the signal, enabling the examination of localized features or changes at different positions. Together, they facilitate comprehensive signal analysis (Mallat, 1999).

According to Figure (1), it can be seen that by using wavelet transformation, the occurrence time of different frequencies can be extracted. Wavelet transform is divided into two categories: discrete and continuous. Wavelet transformation can be discrete or continuous by three parameters: time, scale, and shift.

On the other hand, continuous wavelet transform can also be used for discrete waves in time,

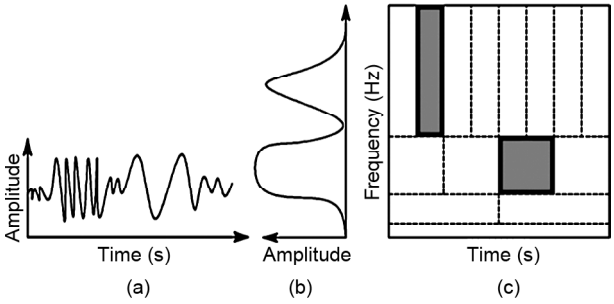

Figure 1. Relationship between time, frequency, and wavelet amplitude. (a) Time-Series, (b) Fourier Spectrum and (c) Wavelet Transform.

in the case that continuous wavelet transform is used for discrete waves, two parameters of scale and shift are actually continuous.

Continuous wavelet transform is mostly used for time-frequency studies, and discrete wavelet transform is used as a filter bank. Continuous wavelet transform is defined according to Equation (1) (Alonso et al., 2004; Jena et al., 2021; Kankanamge et al., 2020; Mallat, 1999; Nagarajaiah & Basu, 2009; Pandit & Sharma, 2020; Pnevmatikos & Hatzigeorgiou, 2017).

$$X_{WT}(\tau,s)=\frac{1}{\sqrt{s}}\int_{-\infty}^{+\infty}x(t)\psi^{*}\left(\frac{t-\tau}{s}\right)dt \qquad (1)$$

In Equation (1), the continuous wavelet transform is obtained based on two parameters of shift (τ) and scale (s). In this relationship, $x(t)$ represents the input wave in terms of time, the mother function is represented by ψ, and also * represents the complexity of the function. As mentioned, the scale and shift parameters change continuously. Considering that in this article, the goal is to reduce the time steps of the earthquake and convert it into two waves with high and low frequencies, so for this purpose, discrete wavelet transformation has been used. In fact, by using discrete wavelet transform, the waves can be divided into a series of low-pass and high-pass filters. Therefore, in this paper, the input wave, scale, and shift are all discrete.

In practice, discrete wavelet transform is implemented as a filter bank. This means that it works as a sequence of low-pass and high-pass filters. According to Figure (2), the number of points is assumed to be N for signal S, which is the earthquake acceleration wave in this article. The S wave is converted into two high-pass (D1) and low-pass (A1) waves using wavelet transformation. The high-pass wave represents the wave of details and the low-pass wave represents the wave of approximations. Due to the fact that the detail wave includes the high frequencies of the earthquake, it can be removed by considering a suitable approximation. By removing the detail wave in each level, the number of input wave points is reduced to half of the previous level. In this way, in each level, the approximation wave can be divided into two parts, low-pass and high-pass, and in the next step, only the low-pass part can be used. In references (Dadkhah et al., 2020; Kamgar et al., 2021; Kamgar et al., 2020; Kamgar et al., 2021; Majidi et al., 2022; Majidi et al., 2022), this method is used as a suitable method to reduce earthquake points. In this article, the earthquake acceleration wave is filtered to five levels using discrete wavelet transform according to the method shown in Figure (2).

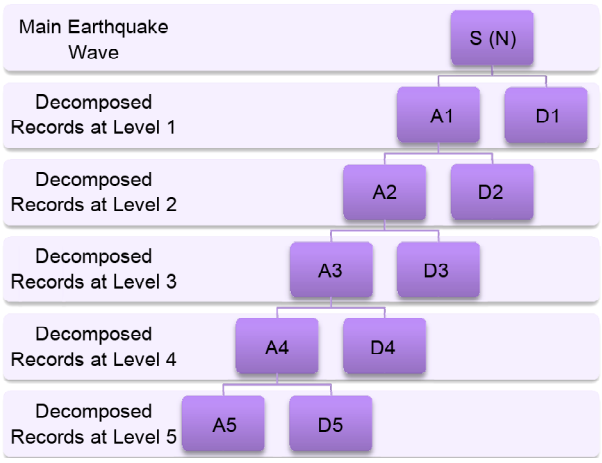

Figure 2. Discrete wavelet transform algorithm.

Due to the fact that wave A is more similar to the main earthquake, this wave is used as a substitute for the main earthquake. Therefore, the number of discrete points for waves A1 to A5 is half, one quarter, one eighth, one-sixteenth, and one thirty-second of the main record of the earthquake, respectively.

To demonstrate the filtering process, one of Chi-Chi earthquake records is examined using the discrete wavelet transform. This record is filtered up to 5 levels using Haar wavelet function. The number of points of this wave is 18,000. At each level of the filter, a wave of approximations and a wave of details is obtained. The number of wave points of wave of approximations and wave of details after the first level of filtering is 9000. Also for the second to the fifth level, the number of points is 4500, 2250, 1125 and 563, respectively. Figure (3) shows the curves of the main earthquake wave and the waves of approximations and details at different levels of filtering. As can be seen in Figure (3), the wave of approximations is very similar to the main wave, both in appearance and amplitude.

In this article, the wavelet functions of the

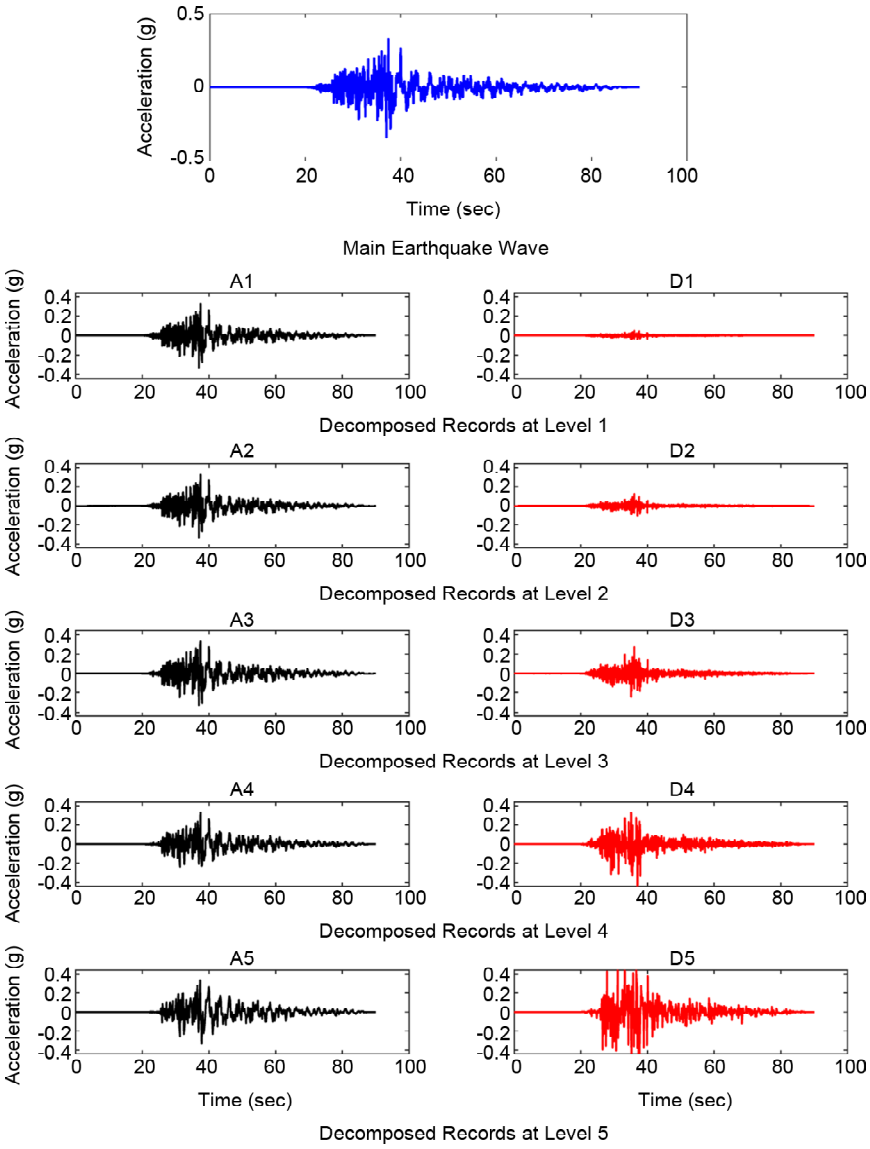

Figure 3. Discrete wavelet transform for Chi-Chi earthquake.

Daubechies and Biorthogonal families are investigated. Previously, only Daubechies 1 and 4 wavelet functions were used in the articles related to this field (Dadkhah et al., 2020; Heidari & Majidi, 2021; Kamgar et al., 2021; Kamgar et al., 2020; Kamgar et al., 2021; Majidi et al., 2022; Majidi, et al., 2022). However, in this article, a complete review of the wavelet functions of the Daubechies family, which includes 10 different wavelet functions, is discussed. The Daubechies wavelet functions are a family of orthogonal wavelet functions. The Daubechies wavelet family is represented by dbN in which N stands for the wavelet order and db stands for Daubechies (Daubechies, 1992).

It should also be noted that db1 is the Haar wavelet functions. The other ten members of this group are shown in Figure (4).

Biorthogonal wavelet functions can be suitable mother functions due to their good properties for finding wavelet coefficients (Majidi et al., 2023). Biorthogonal wavelets possess two key properties: perfect reconstruction and a dual basis. These properties minimize distortion during signal compression and enable efficient representation of both smooth and abrupt signal changes. Perfect reconstruction ensures that the original signal can be accurately reconstructed from its wavelet coefficients. The dual basis property allows for a complementary analysis, facilitating the capture of various signal characteristics with high precision and adaptability, making biorthogonal wavelets widely used in signal processing and data compression applications (Misiti et al., 1996).

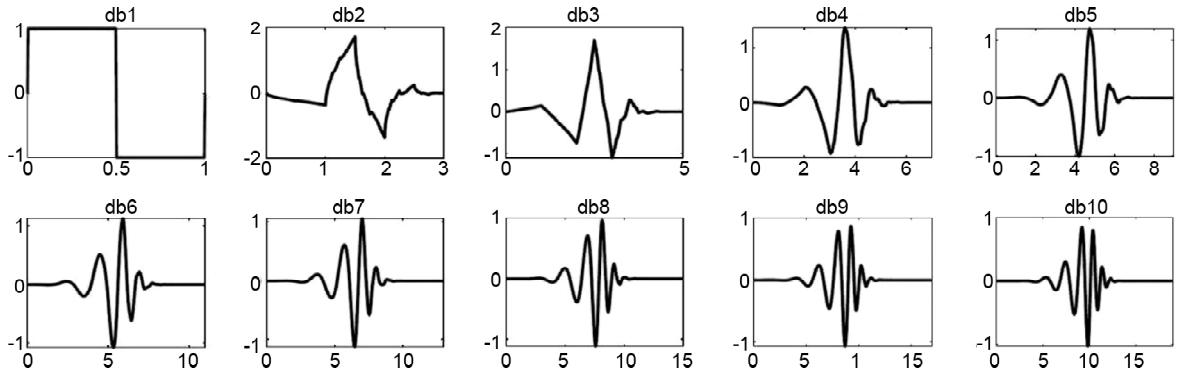

Figure 4. Daubechies Wavelet Functions (schematic illustration).

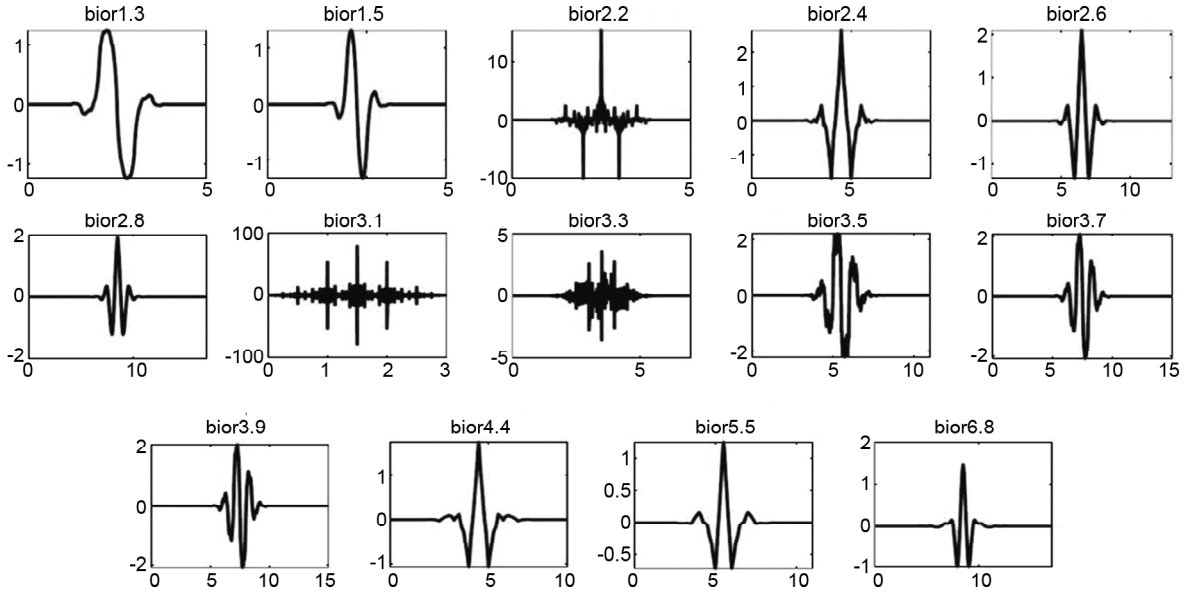

Figure 5. Biorthogonal Wavelet Functions (schematic illustration).

Previously, these wavelet functions have been used in generating artificial earthquake records, damage detection, and earthquake frequency analysis (Hémon & Santi, 2007; Mehr Motlagh et al., 2021; Spanos & Rao, 2001; Teng et al., 2006; Wang et al., 2011). As mentioned, the use of these functions to down-sampling was first proposed by Majidi et al. (Majidi et al., 2023) in 2023 and it was shown that it can reduce the calculation error in the third level of decomposition by more than 3 times. However, in this study, the performance of these functions is investigated in the fourth and fifth levels of decomposition, Figure (5).

The following Table (1) is used to name different mother wavelet functions. Based on the table presented below, wavelet functions WT1 to WT10 are related to Daubechies wavelet functions. Also, functions WT11 to WT24 are related to Biorthogonal wavelet functions.

3. Numerical Methods Used to Analyze Single Degree of Freedom Systems

The Figure (6) shows an ideal mass-spring single degree of freedom system. The displacement equation of this system is obtained using the following relationship. In the vibrating system, when the mass is moved by the amount u, the elastic stretching of the column (spring tension) is used to return the mass to its initial position, this force (f_s) in the column or spring is a function of the displacement u is called spring stiffness. If the system is elastic and there is no loss of energy, the mass will vibrate forever, but in practice, friction with the air, friction between the system particles or in the connections, yielding of materials and the formation of cracks and friction between them causes the loss of vibration energy. Forces that cause energy loss(f_D) are known as damping (depreciation) forces.

Table 1. 24 mother wavelet functions used in this study.

Mother Wavelet Function	Symbol	Mother Wavelet Function	Symbol
db1	WT1	bior2.2	WT13
db2	WT2	bior2.4	WT14
db3	WT3	bior2.6	WT15
db4	WT4	bior2.8	WT16
db5	WT5	bior3.1	WT17
db6	WT6	bior3.3	WT18
db7	WT7	bior3.5	WT19
db8	WT8	bior3.7	WT20
db9	WT9	bior3.9	WT21
db10	WT10	bior4.4	WT22
bior1.3	WT11	bior5.5	WT23
bior1.5	WT12	bior6.8	WT24

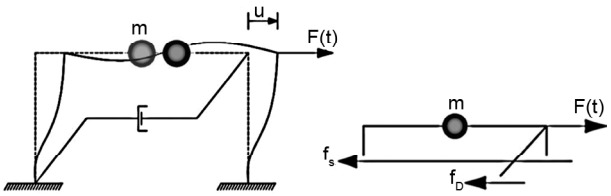

Figure 6. Effective dynamic forces in a single degree of freedom systems.

In Equation (2), parameters *m*, *c* and *k* represent mass, damping and stiffness, respectively. Also, in this equation, $F(t)$ represents the external force in terms of time.

$$m\ddot{u} + c\dot{u} + ku = F(t) \tag{2}$$

Numerical methods are suggested to solve the vibration equation for various types of dynamic loading, especially if the force does not have a specific mathematical function.

Numerical methods for solving vibration equations are divided into three categories, which include methods based on excitation function interpolation, methods based on finite difference, and methods based on acceleration changes (Clough & Penzien, 1975; Hilber, 1976). This article reduces calculation costs by extending the earthquake's time step. Thus, methods of unconditional stability should be employed.

Therefore, in this article, methods based on interpolation (Nigam & Jennings, 1968, 1969) and the Newmark's average acceleration method, which is a method based on changes in acceleration, are used. In the following, the relationships related to considering linear interpolation between the earthquake data are presented in a summary form. Displacement and velocity are obtained from Equations (3) and (4), respectively (Chopra, 2012).

$$u_{i+1} = Ap_i + Bp_{i+1} + Cu_i + D\dot{u}_i \tag{3}$$

$$\dot{u}_{i+1} = A'p_i + B'p_{i+1} + C'u_i + D'\dot{u}_i \tag{4}$$

Also, the coefficients related to Equations (3) and (4) are obtained from the following relations.

$$A = \frac{1}{k}\left\{\frac{2\xi}{\omega\Delta t} + e^{-\xi\omega\,\Delta t}\left[\left(\frac{1-2\xi^2}{\omega_D\,\Delta t} - \frac{\xi}{\sqrt{1-\xi^2}}\right)\times \sin\omega_D\,\Delta t - \left(1+\frac{2\xi}{\omega\Delta t}\right)\cos\omega_D\,\Delta t\right]\right\} \tag{5}$$

$$B = \frac{1}{k}\left[1 - \frac{2\xi}{\omega\Delta t} + e^{-\xi\omega\Delta t}\times \left(\frac{2\xi^2-1}{\omega_D\Delta t}\sin\omega_D\Delta t + \frac{2\xi}{\omega\Delta t}\cos\omega_D\Delta t\right)\right] \tag{6}$$

$$C = e^{-\xi\omega\Delta t}\left(\frac{\xi}{\sqrt{1-\xi^2}}\sin\omega_D\Delta t + \cos\omega_D\Delta t\right)\times$$
$$D = e^{-\xi\omega\Delta t}\left(\frac{1}{\omega_D}\sin\omega_D\Delta t\right) \tag{7}$$

$$A' = \frac{1}{k}\left\{-\frac{1}{\Delta t} + e^{-\xi\omega\Delta t}\left[\left(\frac{\omega}{\sqrt{1-\xi^2}} + \frac{\xi}{\Delta t\sqrt{1-\xi^2}}\right)\times \sin\omega_D\Delta t + \frac{1}{\Delta t}\cos\omega_D\Delta t\right]\right\} \tag{8}$$

$$B' = \frac{1}{k\Delta t}\times \left[1 - e^{-\xi\omega\Delta t}\left(\frac{\xi}{\sqrt{1-\xi^2}}\sin\omega_D\Delta t + \cos\omega_D\Delta t\right)\right] \tag{9}$$

$$C' = -e^{-\xi\omega\Delta t}\left(\frac{\omega}{\sqrt{1-\xi^2}}\sin\omega_D\Delta t\right).$$
$$D' = e^{-\xi\omega\Delta t}\left(\cos\omega_D\Delta t - \frac{\xi}{\sqrt{1-\xi^2}}\sin\omega_D\Delta t\right) \tag{10}$$

In the above relationships, the parameters *k*, ω, ξ and Δt are stiffness, natural frequency, damping,

and time step respectively. Also, the second method used in this article is Newmark's average acceleration method, which is based on the following relationships. In this method, γ and β parameters are considered as 0.5 and 0.25, respectively (Chopra, 2012).

$$\dot{u}_{i+1} = \dot{u}_i + [(1-\gamma)\Delta t]\,\ddot{u}_i + (\gamma\,\Delta t)\,\ddot{u}_{i+1} \tag{11}$$

$$u_{i+1} = u_i + (\Delta t)\,\dot{u}_i + [(0.5-\beta)(\Delta t)^2]\,\ddot{u}_i + [(\beta(\Delta t)^2]\,\ddot{u}_{i+1} \tag{12}$$

4. Selected Earthquake Records

In this paper, the records provided by FEMA P695 (Council, 2000) are used for dynamic analysis. The records used in this article include the recorded earthquakes in the far-field, near-field, and with pulse. The magnitudes of the selected earthquakes are between 6 and 8 on the Richter scale. Also, the acceleration of most selected earthquakes is from 0.11 g to 2 g. In the Table (2), the characteristics of 50 earthquakes used in this article are presented.

5. Analysis of Single Degree of Freedom Systems with Different Wave Functions

In this part, to check the performance of different wavelet functions, the response of the single degree of freedom systems is investigated. In this article, 201 single-degree of freedom structures with a period between 0.05 seconds and 10 seconds are analyzed. Therefore, by examining 50 earthquake records and 201 single-degree-of-freedom structures, more than 10,000 analyzes have been performed for each wave. The results presented in previous researches have shown that if a mother function is suitable for linear analysis, if the numerical method is stable, it is also stable for the nonlinear case (Dadkhah et al., 2020; Heidari & Majidi, 2021; Heidari et al., 2019; Kamgar et al., 2021; Kamgar et al., 2020; Kamgar et al., 2021). Therefore, in this article, only the linear mode method of different wavelet functions is discussed. In this study, each earthquake is filtered up to 5 steps. Based on what was said, in each stage of the filter, the number of recorded points is reduced to half of the previous stage. This issue makes it possible to increase the time step of the analysis to the time step of the approximate waves obtained from the wavelet method, if there are no limitations related to the time step of the numerical method. In order to have a comprehensive study, in this article 24 mother wavelet functions, 50 earthquakes, 201 single degree of freedom systems and 5 approximate waves for each earthquake have been examined. All these analyses have been performed for both Newmark's average acceleration and interpolation numerical methods. At first, for the initial investigation of the effect of the wavelet function on the calculation error, the average error rate for 50 earthquakes and 201 periods is obtained from the following relationship. In the following relationship, $S_{ie,Main}$ is the value of the acceleration response spectrum obtained from the main earthquake records in the i-th period for earthquake *e* and $S_{ie,Ax}$ is the corresponding value obtained from the approximate wave. In this article, Ax can be A1, A2, A3, A4 or A5. In the following relationships, *n* is the number of single-degree of freedom systems of each spectrum and *E* is the number of earthquakes.

$$Er_{mean} = \left| \left(\left(\frac{1}{E} \frac{1}{n} \right) \sum_{e=1}^{E} \sum_{i=1}^{n} \frac{S_{ie,Main} - S_{ie,Ax}}{S_{ie,Main}} \right) \right| \times 100 \qquad E = 50,\ \ n = 201 \tag{13}$$

Based on Equation (13), the following figure is presented for the error of different mother wavelet functions and different numerical methods. In previous studies from 2002 until now, the wavelet method was used to reduce the sampling of earthquake waves from the wavelet functions db1 and db4 (Dadkhah et al., 2020; Kamgar et al., 2020; Kamgar, et al., 2021; Majidi et al., 2022). In all these studies, the A3 wave has been suggested as a suitable approximation to reduce the maximum cost of calculations, with a negligible error. However, in none of the studies, more than 20 earthquakes have been investigated. Also, in some of these studies, the A3 wave error has reached more than 70% in some structures (Heidari et al., 2019; Kamgar et al., 2021). Therefore, it can be concluded that perhaps one of the reasons for the error in these structures was the inappropriate choice of the wavelet function. Based on a study

Table 2. Characteristics of selected earthquakes.

Record Number	NGA Record Number	Earthquake Name	Station Name	Type
1	68	San Fernando	LA - Hollywood Stor FF	FF
2	125	Friuli, Italy-01	Tolmezzo	FF
3	126	Gazli, USSR	Karakyr	NF
4	160	Imperial Valley-06	Bonds Corner	NF
5	165	Imperial Valley-06	Chihuahua	NF
6	169	Imperial Valley-06	Delta	FF
7	174	Imperial Valley-06	El Centro Array #11	FF
8	181	Imperial Valley-06	El Centro Array #6	NFP
9	182	Imperial Valley-06	El Centro Array #7	NFP
10	292	Irpinia, Italy-01	Sturno (STN)	NFP
11	495	Nahanni, Canada	Site 1	NF
12	496	Nahanni, Canada	Site 2	NF
13	721	Superstition Hills-02	El Centro Imp. Co. Cent	FF
14	723	Superstition Hills-02	Parachute Test Site	NFP
15	725	Superstition Hills-02	Poe Road (temp)	FF
16	741	Loma Prieta	BRAN	NF
17	752	Loma Prieta	Capitola	FF
18	753	Loma Prieta	Corralitos	NF
19	767	Loma Prieta	Gilroy Array #3	FF
20	802	Loma Prieta	Saratoga-Aloha Ave	NFP
21	821	Erzincan, Turkey	Erzincan	NF
22	825	Cape Mendocino	Cape Mendocino	NF
23	827	Cape Mendocino	Fortuna - Fortuna Blvd	FF
24	828	Cape Mendocino	Petrolia	NFP
25	848	Landers	Coolwater	FF
26	879	Landers	Lucerne	NFP
27	900	Landers	Yermo Fire Station	FF
28	953	Northridge-01	Beverly Hills-Mulhol	FF
29	960	Northridge-01	C. Country-W Lost Cany	FF
30	1004	Northridge-01	LA-Sepulveda VA Hospital	NF
31	1048	Northridge-01	Northridge-17645 Saticoy St	NF
32	1063	Northridge-01	Rinaldi Receiving Sta	NFP
33	1086	Northridge-01	Sylmar-Olive View Med FF	NFP
34	1111	Kobe, Japan	Nishi-Akashi	FF
35	1116	Kobe, Japan	Shin-Osaka	FF
36	1148	Kocaeli, Turkey	Arcelik	FF
37	1158	Kocaeli, Turkey	Duzce	FF
38	1165	Kocaeli, Turkey	Izmit	NFP
39	1176	Kocaeli, Turkey	Yarimca	NF
40	1244	Chi-Chi, Taiwan	CHY101	FF
41	1485	Chi-Chi, Taiwan	TCU045	FF
42	1503	Chi-Chi, Taiwan	TCU065	NFP
43	1504	Chi-Chi, Taiwan	TCU067	NF
44	1517	Chi-Chi, Taiwan	TCU084	NF
45	1529	Chi-Chi, Taiwan	TCU102	NFP
46	1602	Duzce, Turkey	Bolu	FF
47	1605	Duzce, Turkey	Duzce	NFP
48	1633	Manjil, Iran	Abbar	FF
49	1787	Hector Mine	Hector	FF
50	2114	Denali, Alaska	TAPS Pump Station #10	NF

conducted on 10,000 single degree of freedom systems, according to Figure (7), it can be concluded that db1 and db4 are not very suitable functions for down-sampling of earthquake records. The error of the A3 wave for these functions is about 20% and 14%, respectively. Based on Figure (6), it can be concluded that A3 waves obtained from Daubechies wavelet functions are not very accurate. In most cases, the error of these functions for the A3 wave is more than 13%. Meanwhile, the approximate waves obtained from Biorthogonal wavelet functions work well in most cases.

According to Figure (3), it can be said that the functions WT13 to WT21 have negligible error. The error of these functions for making the A3 wave is less than 7%. However, the best wavelet function for constructing the approximate A3 wavelet is the bior2.6 wavelet function. The error that this wavelet function introduces into the calculations to make the approximate A3 wave is about 2.5%. On the other hand, the best wavelet function for making the approximate wave A1 and A2 is bior6.8 and bior2.4, respectively. The error that these functions enter into the calculations to make the approximate wave A1 and A2 is 0.7 and 0.3 percent, respectively. In the studies conducted in the past, the last reliable stage for making an approximate wave, the third stage (A3), has been introduced. But the results presented in this article show that in the fourth stage of wave decomposition (A4) dynamic analysis can be done accurately by choosing the appropriate wavelet function. In fact, if the A4 wave is made using the appropriate wavelet function, it can introduce an error of less than 2% into the calculations.

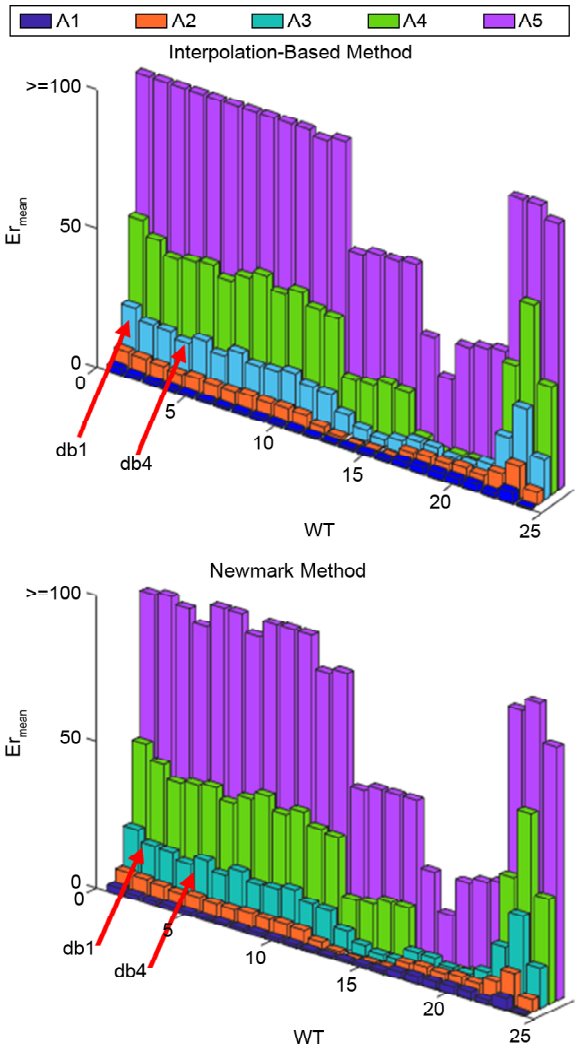

Figure 7. Calculation error for different wave functions and different numerical methods.

Based on the error criterion presented in Equation (13), the best wavelet function and its error for different numerical methods and different approximate waves are presented in the Table (3). According to the results presented in the Table (3), it can be concluded that the best wavelet function is the same in both numerical methods for different approximate waves. On the other hand, for all approximate waves A1 to A5, the best wavelet function was from the Biorthogonal family. In other words, the family of Daubechies wavelet functions that have been proposed in various studies in these 20 years has not performed the best in any of the wavelet transform decomposition levels. Also, based on the results presented in the table below, it can be concluded that the Newmark's average acceleration method has fewer errors.

If the wavelet transform is considered as a smart way to remove the high frequencies of the wave, it can be said that the accuracy of each wavelet function can be recognized from the Fourier spectrum. For this purpose, the average Fourier spectrum of 50 earthquakes for the wavelet

Table 3. The best wavelet function for different approximate wavelets.

Wave	Interpolation-Based Method		Newmark Method	
	Best Wavelet Function	Er_{mean}	Best Wavelet Function	Er_{mean}
A1	bior6.8	0.71	bior6.8	0.66
A2	bior2.4	0.27	bior2.4	0.29
A3	bior2.6	2.59	bior2.6	2.25
A4	bior3.3	2.76	bior3.3	1.54
A5	bior3.3	26.98	bior3.3	18.44

functions db1 and db4 proposed in previous studies and the wavelet functions presented in Table (3) are examined.

Due to the high error of wave A5, the results are presented only for waves A1 to A4. Based on the results presented in Figures (8) and (9), it can

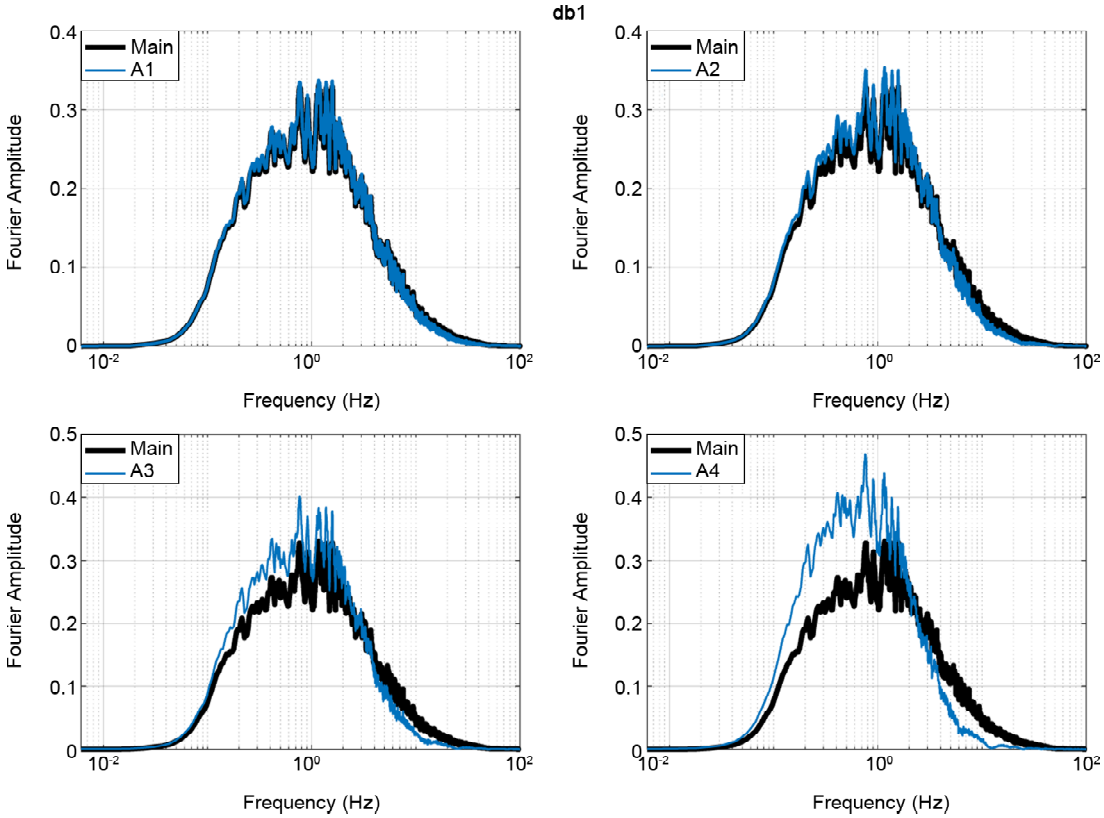

Figure 8. The average Fourier spectrum of the approximate waves obtained from the db1 wavelet function.

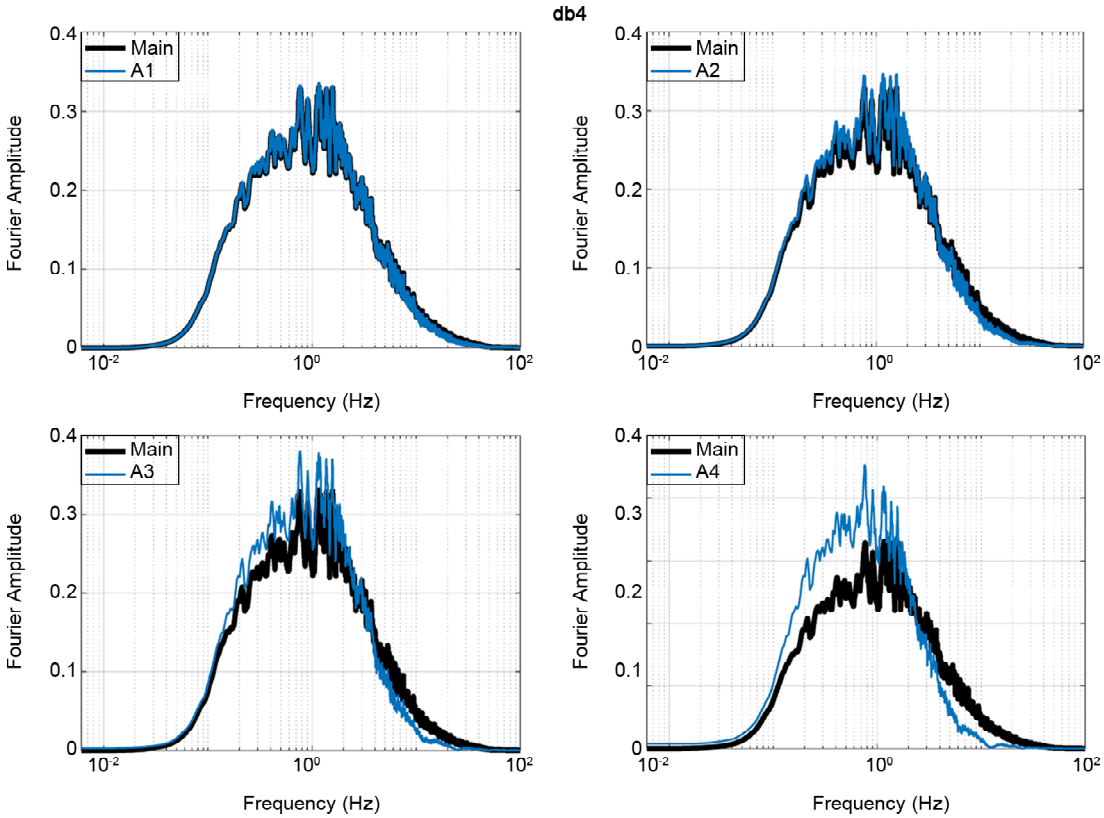

Figure 9. The average Fourier spectrum of the approximate waves obtained from the db4 wavelet function.

be seen that the approximate waves A3 and A4 obtained from the functions db1 and db4 do not have proper accuracy. In other words, the results obtained from these functions are only acceptable for A1 and A2. On the other hand, based on Figure (10), it can be seen that the proposed wavelet functions for each level of approximate wave decomposition have appropriate accuracy. Therefore, the frequency content of the approximate waves A1 to A4 is preserved by using the proposed wavelet functions.

In order to show the effect of the wavelet function on the calculation error of single degree of freedom systems, in the continuation of the average spectrum error of 50 earthquakes for the wavelet functions db1 and db4 that were proposed in previous studies and the average spectrum error for the functions presented in table 3 according to the relationship of 14 cases is reviewed. In the following relationship, parameters $S_{i,Main}$ and $S_{i,Ax}$ are respectively the average spectral response for the spectrum obtained from main earthquakes and the spectrum obtained from approximate earthquakes. As shown in the graphs presented in Figure (7), the A5 wave has an error of more than 18% for all wavelet functions, so it can be said that this wave is not suitable for dynamic analysis.

Therefore, the results for the approximate waves A1 to A4 and the Newmark's average acceleration method, which had less error, are presented below.

$$Error_{Spec}\,(\%) = \left| \frac{S_{i,Main} - S_{i,Aj}}{S_{i,Main}} \right| \times 100 \tag{14}$$

The Figure (11) shows the calculation error curve for two wavelet functions db1 and db4. As can be seen, the calculation error is negligible only for waves A1 and A2 with an error of about 1% and 4%. The calculation error of A3 and A4 waves in these functions is about 20% and 50% for most structures. Therefore, these functions can only be used to make approximate waves A1 and A2. This conclusion is contrary to the claims made in previous articles. In previous studies that have been conducted on a limited number of earthquakes (often less than 5 earthquakes), the last suitable filter stage for these wavelet functions, the third stage filter (A3), has been reported. But the results presented in this article do not confirm this issue.

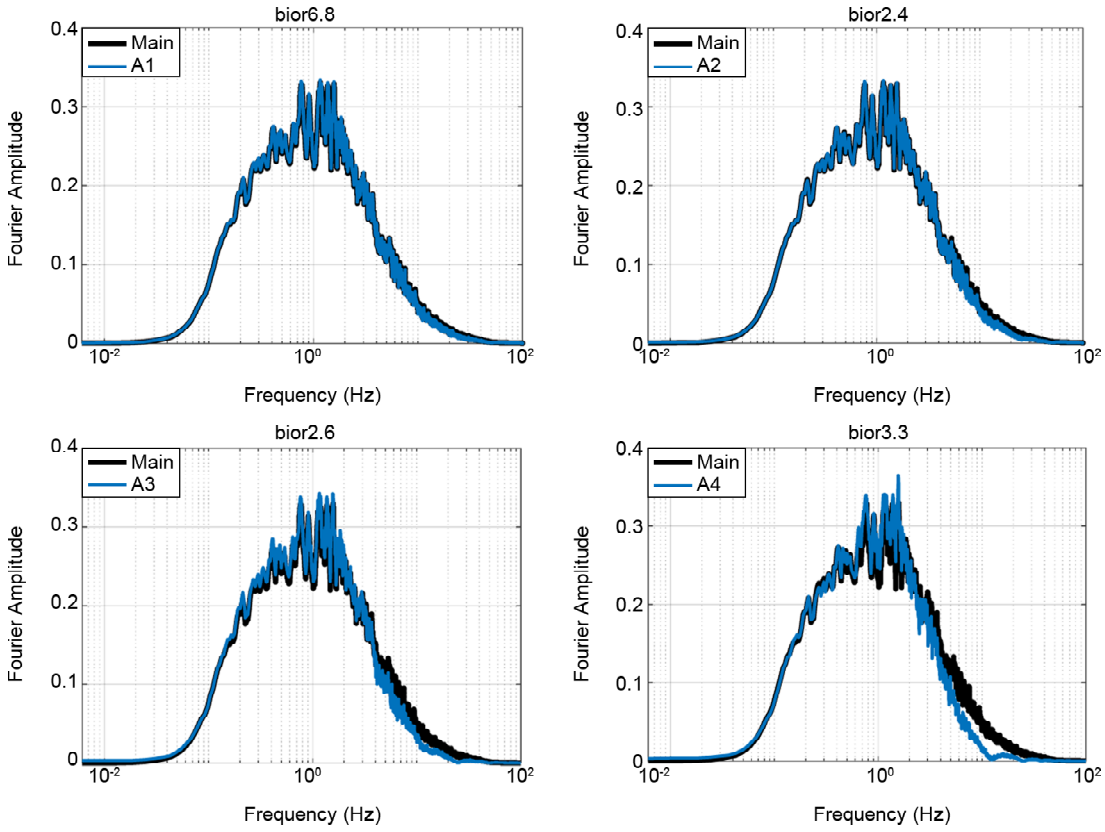

Figure 10. The average Fourier spectrum of the approximate waves obtained from the wavelet functions presented in Table (3).

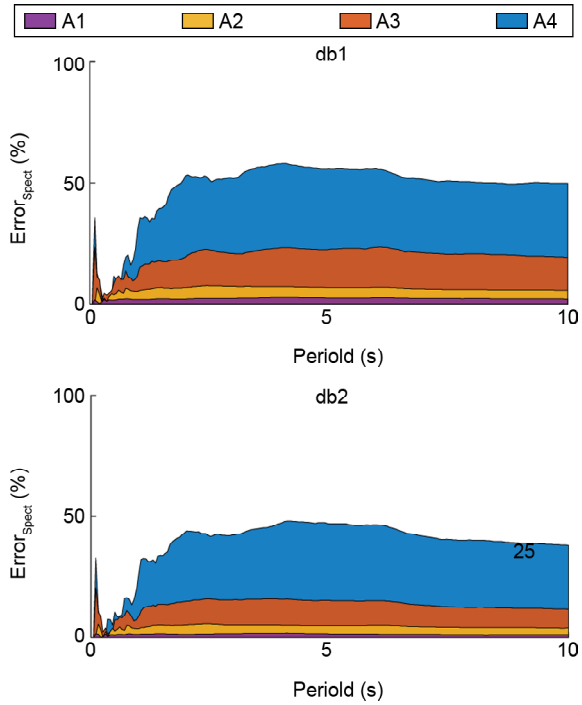

Figure 11. Average spectrum error curve for db1 and db4 wavelet functions.

In the following, the average spectrum error results for the wavelet functions presented in Table (3) have been examined. Based on the results presented in the following Figure (12) for the average spectrum error, it can be concluded that the wavelet function bior6.8 with an error of less than 1% is suitable for making approximate A1 waves. The bior2.4 wavelet function is also suitable for making A1, A2 and A3 approximate waves with a lower error of 1.5%, 0.5% and 4%. Also, the bior2.6 wavelet function is also suitable for making A1, A2 and A3 approximate waves with less error of 1.5%, 0.7% and 2.5%. None of the bior2.4 and bior2.6 functions are suitable for making the approximate A4 wave. But the wavelet function of bior3.3 with an error of about 3%, 5%, 7% and 1.5% is suitable for making all the approximate waves of A1, A2, A3 and A4.

In the following, the average acceleration response spectrum of 50 earthquakes for wavelet functions db1 and db4 proposed in previous studies and wavelet functions presented in Table (3) are examined. Due to the high error of wave A5, the results are presented only for waves A1 to A4.

Based on the results presented in the Fgures (13) to (15), it can also be said that the wavelet

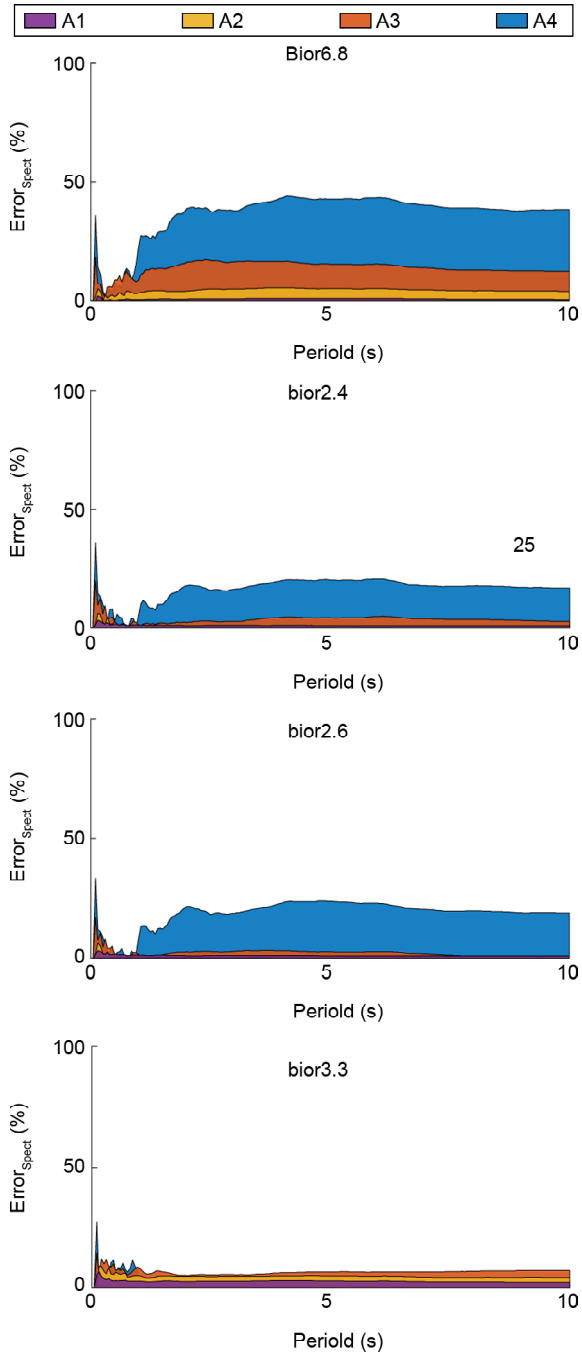

Figure 12. Average spectrum error for wavelet functions Table (3).

functions db1 and db4 are only suitable for making approximate waves A1 and A2. Also, the results presented in Figure (14) show that choosing the appropriate wavelet function for each level of decomposition can lead to an increase in the accuracy of calculations in dynamic analysis.

6. Analysis of a 20-Story Structure

In the following, to investigate the effect of the wavelet function on the accuracy of the calculations, the nonlinear response of the 20-story

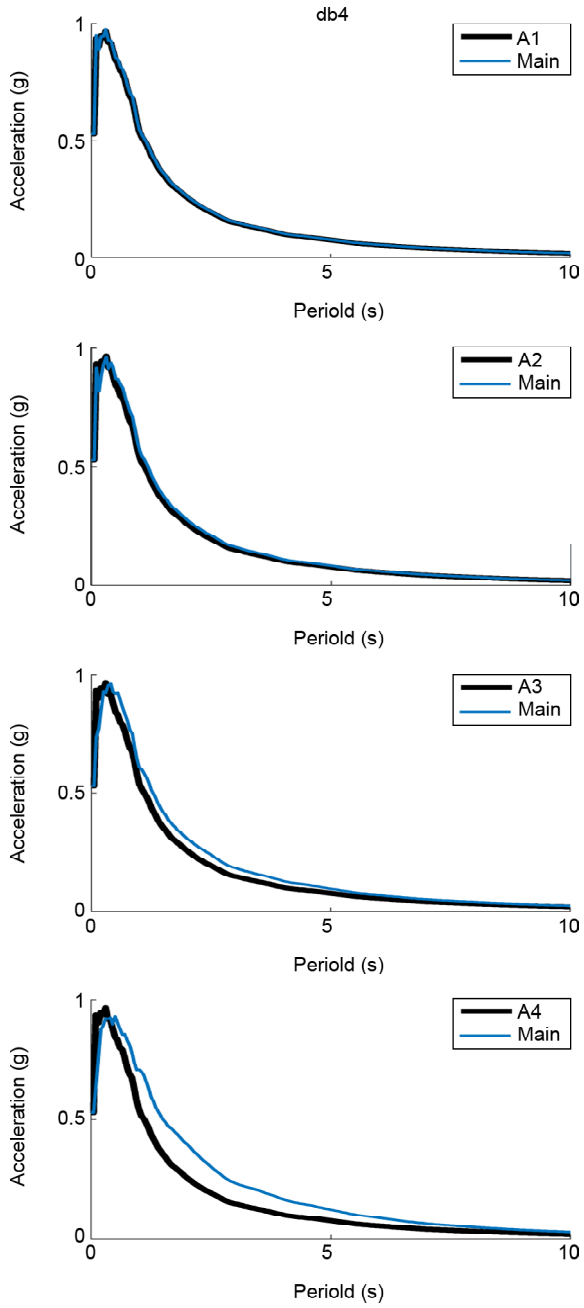

Figure 13. Average acceleration response spectrum of approximate waves obtained from wavelet function db1.

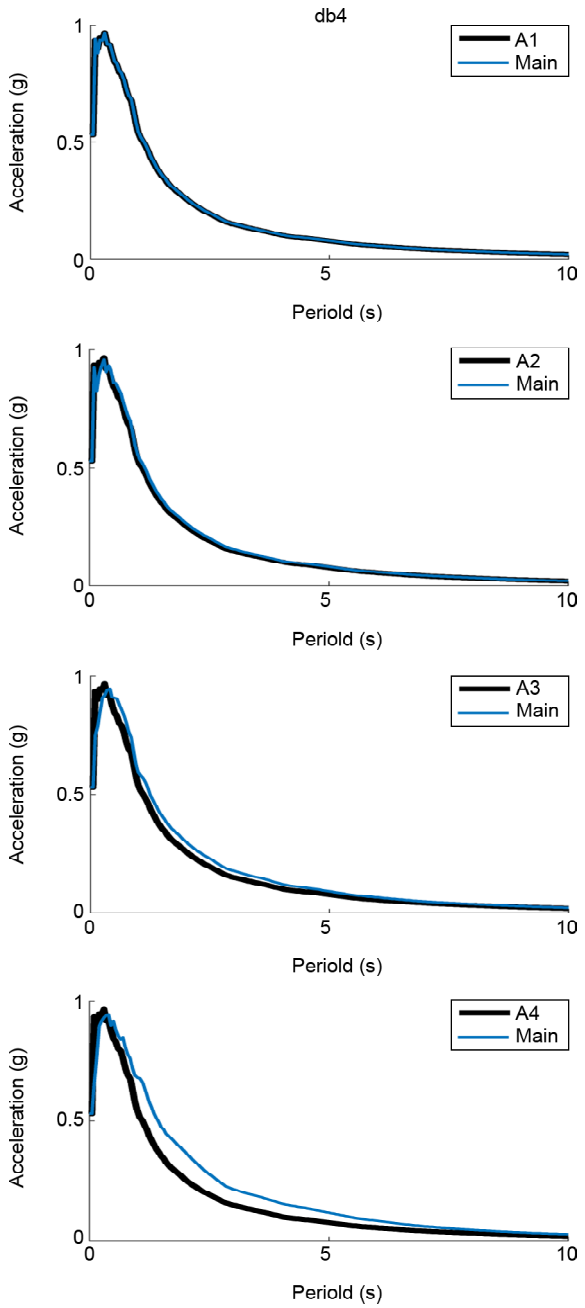

Figure 14. Average acceleration response spectrum of approximate waves obtained from wavelet function db4.

structure of SAC is investigated (Venture, 2000). SAC frames have been used in many articles to carry out studies on structures (Bitaraf et al., 2012; Ghaffary & Moustafa, 2021; Hossain et al., 2013; Jia et al., 2018; Nasab & Kim, 2020; Qiu et al., 2020; Sepasdar et al., 2019; Shayanfar et al., 2016). These structures include 3-story, 9-story, and 20-story. The period of the first natural mode of these structures is 1, 2.34 and 4 seconds, respectively. In the investigation of single degree of freedom systems, it was shown that the accuracy of this category of methods depends on the period of the structure. On the other hand, according to Figures (11) and (12), it was shown that the maximum error occurs in a period of about 4 seconds. In this article, the 20-story structure is used to evaluate the effect of wavelet functions on the nonlinear response of the structure. OpenSees software is used to model the structures. The structures selected in this paper are two-dimensional bending frames designed according to the 1994 UBC design requirements (Gupta & Krawinkler, 1998; Venture, 2000). The structure is shown schematically in the Figure (16). For more

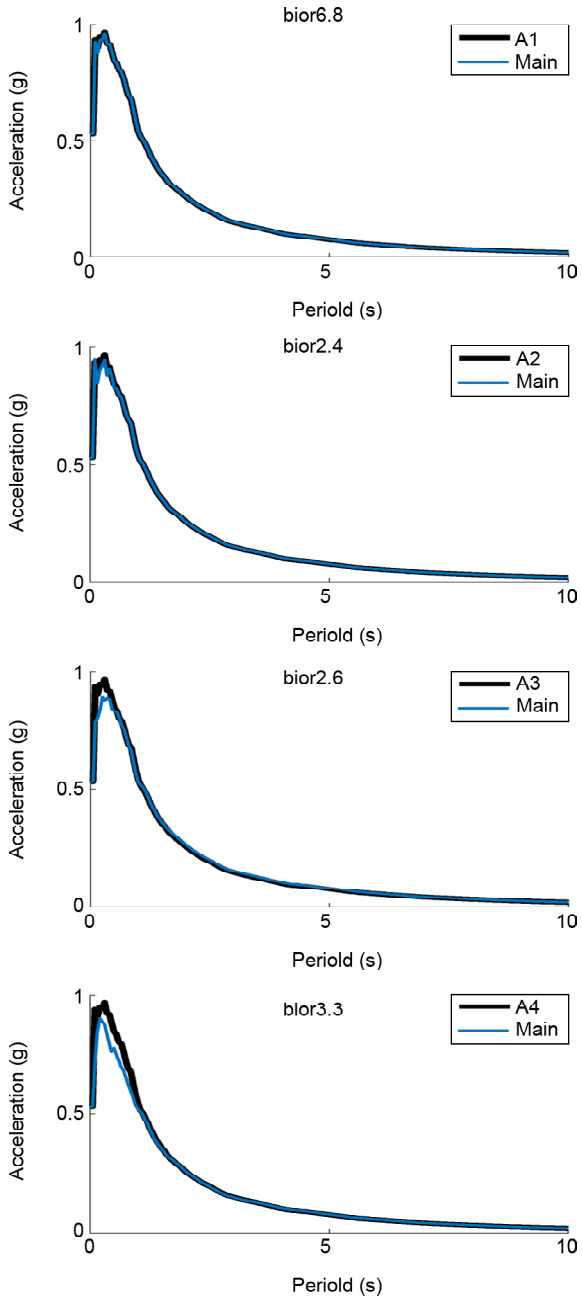

Figure 15. Average acceleration response spectrum of approximate waves obtained from wavelet functions presented in Table (3).

information on the details of the structures, refer to (Venture, 2000).

As mentioned in this paper, OpenSees software is used to model structures for nonlinear dynamic analysis of structures. One of the default materials (Steel 01) has been used to model the behavior of materials. The strain stress curve for steel 01 is as shown in Figure (2). Also, the hardening model of this material is kinematic (Mazzoni et al., 2006). Damping parameters of the structure are also obtained based on the Rayleigh method. To model structural components, sections were considered

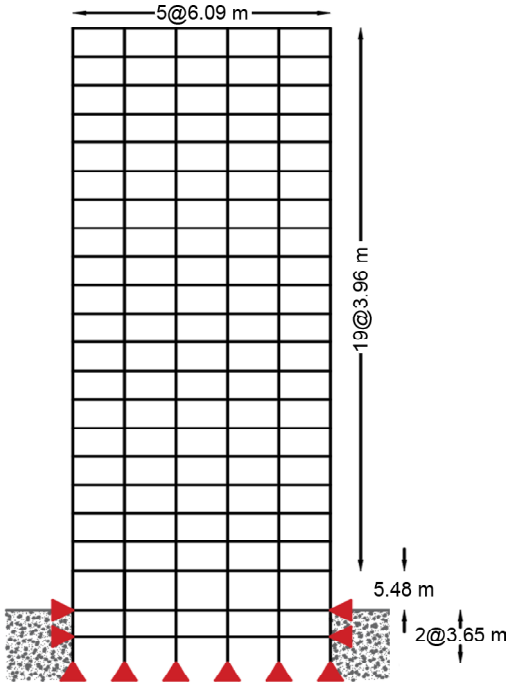

Figure 16. View of the 20-story SAC structure.

as fibers. Also, Newton-Raphson was chosen as the algorithm used for iterative nonlinear analysis. The value of tolerance in the nonlinear solution was also considered 10^{-8}.

In the Figure (17), the parameters F_y, E_0, and b represent the yield stress, modulus of elasticity, and strain-stiffness ratio, respectively. In this paper, the yield stresses for the beams and columns are 3.39×10^5 KN/m^2 and 3.97×10^5 KN/m^2, respectively. The modulus of elasticity for beams and columns 2.00×10^8 KN/m^2 is also considered. Parameter b is also assumed to be 0.0001 for beams and columns. In this article, due to the fact that earthquakes have different PGAs and frequency content, it can be said that the investigated earthquakes include different intensities. In the following, the response spectrum of different earthquakes and the average mean response spectrum are presented, Figure (18).

To check the performance of different wavelet functions in multi-degree-of-freedom structures, three criteria are checked. These three criteria include maximum roof displacement error, story drift error, and foundation cut error. To obtain the said error criteria, Equations (15) to (18) are presented.

$$Er_{D_i}(\%)=\left|\frac{Md_i-Ad_i}{Md_i}\right|\times100 \qquad (15)$$

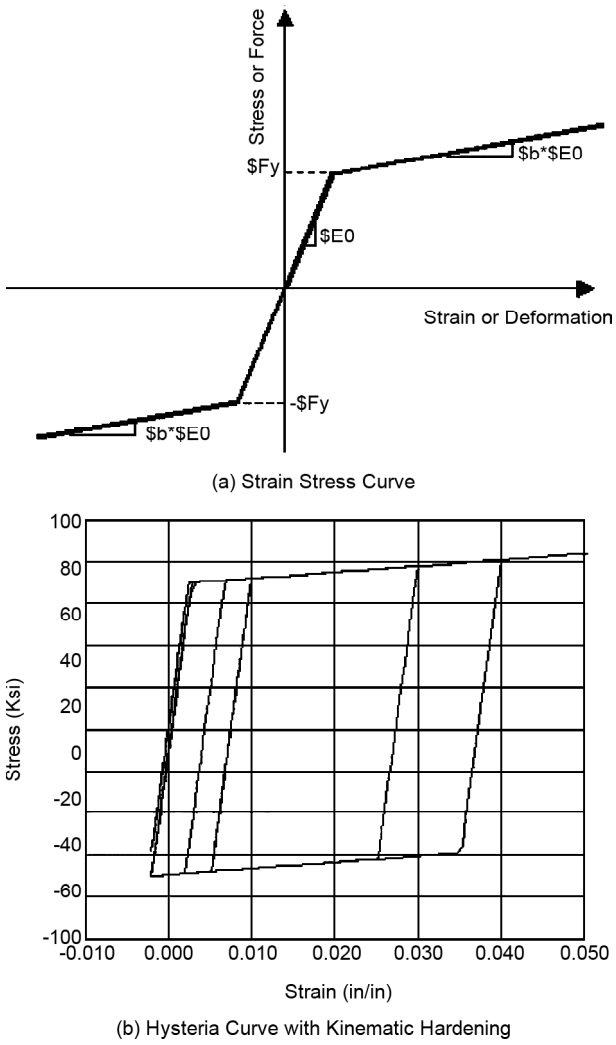

Figure 17. A behavioral model of steel 01 (Mazzoni et al., 2006).

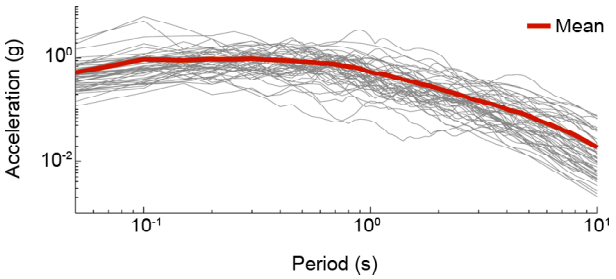

Figure 18. Response spectrum of earthquakes and mean response spectrum.

$$EDr_{ij}\,(\%) = \left|\frac{Mdr_{ij} - Adr_{ij}}{Mdr_{ij}}\right| \times 100 \tag{16}$$

$$Er_{Dr_i}\,(\%) = \frac{1}{S}\sum_{j=1}^{S} EDr_{ij} \tag{17}$$

$$Er_{B_i}\,(\%) = \left|\frac{Mb_i - Ab_i}{Mb_i}\right| \times 100 \tag{18}$$

In the above equations, i and j are the earthquake counter and the story of the desired structure, respectively. Also Md_i, Ad_i, Mdr_{ij}, Adr_{ij}, Mb_i and Ab_i, respectively, the amount of roof displacement for the main wave of the earthquake i, the displacement of the roof for the approximate wave of the earthquake i, the drift of the story j for the earthquake i for the main wave, the drift of the story j for earthquake i for the approximate wave, base shear for the main wave of the earthquake i and base shear for the approximate wave of the earthquake i. Parameters N and S indicate the number of earthquakes and the number of story of the structure. In this article, N and S are equal to 50 and 20, respectively. The parameters Er_{Di}, EDr_{ij}, Er_{Dr_i}, and Er_{B_i}, respectively, indicate the displacement error of the roof for the desired earthquake in a structure, the drift error for the story j and for earthquake i, average drift error of all stories for earthquake i and base shear error for earthquake i in the structure.

Before the error of different earthquakes is examined, the median drift curve and average mean drift curve are examined. Also, in this structure, according to Fema-356, the amount of drift for the IO level is from 0 to 0.7%, for the LS level from 0.7 to 2.5%, and for the CP level from 2.5 to 5% (Council, 2000). The earthquakes studied in this article consider all seismic levels. Therefore, the maximum floor drift is between 0.1% and about 6%. In Figure (19), the average mean drift and median drift curves for different wavelet functions are shown.

The results obtained from Figure (19) confirm this fact that in the analysis performed by the approximate wave A4 obtained from the wavelet functions db1, db4, bior6.8, bior2.4 and bior2.6, the analysis diverges in many cases and also leads to providing large values for drift. In fact, the results of the analysis for the A4 wave obtained from these functions have caused the divergence of the analysis in most cases. Also, the results presented in Figure (20) show that A3 and A4 waves obtained from wavelet functions db1, db4 and bior6.8 do not have proper accuracy. It can also be seen from this figure that the wave A1 to A3 obtained from bior2.4 and bior2.6 has a good accuracy. All the approximate waves obtained

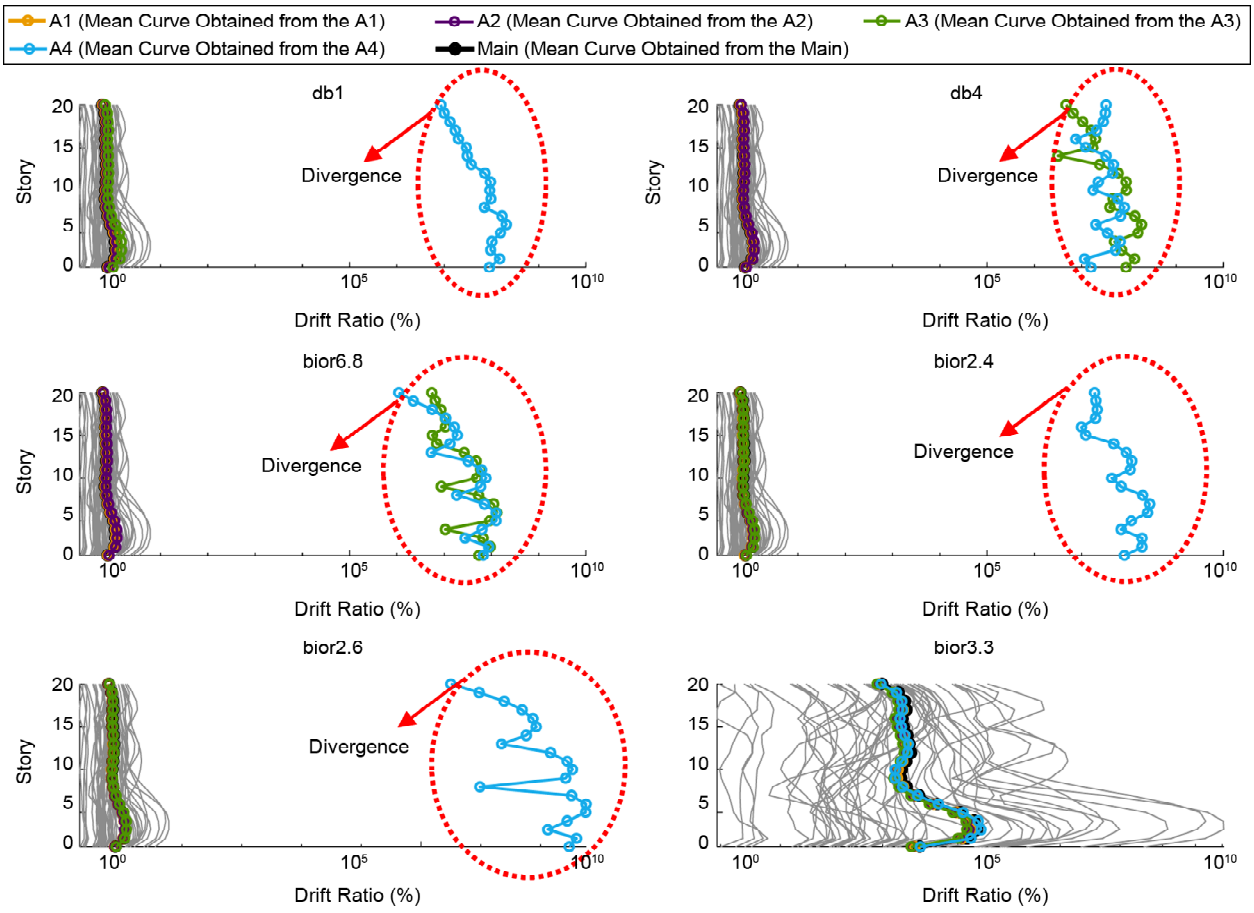

Figure 19. Mean drift curve for different wavelet functions.

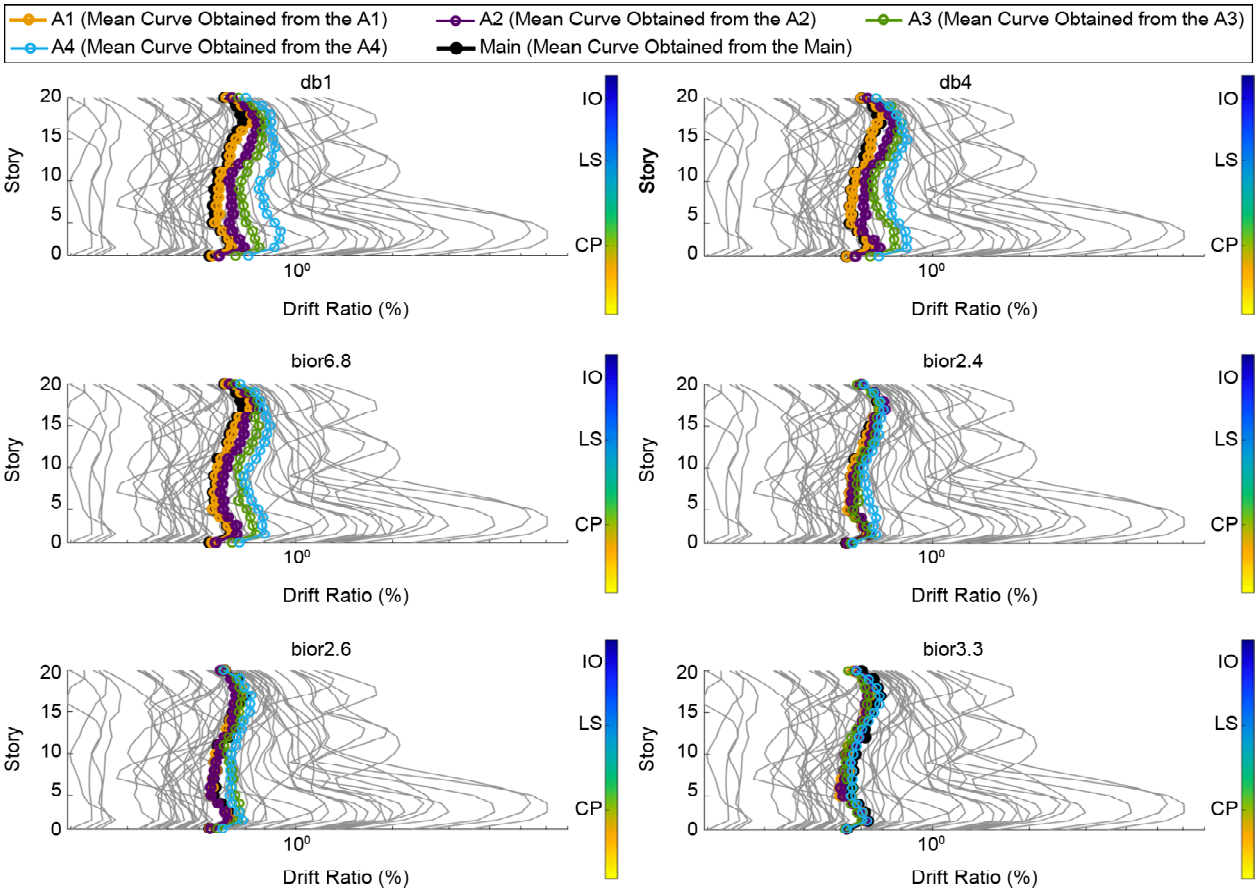

Figure 20. Median drift curve for different wavelet functions.

from the wavelet function of bior3.3 have good accuracy. Figures (19) and (20) show that both the mean drift and the median drift for the approximate waves obtained from the wavelet function bior3.3 have good accuracy.

In the following, displacement error, drift error and base shear error for different earthquakes are shown. As shown in the Figure (21), the error of waves A3 and A4 is higher than the rest of the waves in all functions. According to the Figures (21) to (23), it can be seen that all the error criteria are close to each other in most cases. However, the base shear error is less than the others. For better conclusions about different wavelet functions, the cumulative distribution function (CDF) curve for the drift error is presented below. In the Figure (24), the CDF curve for different wavelet functions is presented.

According to Figure (24), it can be seen that the wavelet functions db1 and db4 are only suitable for making approximate waves A1 and A2. Based on the required accuracy, the best wavelet function can be determined statistically from the analyses performed. If the error of 5% is considered as the maximum calculation error, the best wavelet functions for constructing the approximate wave A1 are the wavelet functions bior6.8, bior2.4 and bior2.6. Also, based on this error, the best wavelet function for making the approximate wave A2 is the wavelet function bior2.4. For making the approximate wave A3, the best wavelet function is bior2.6. Based on the maximum error of 5%, the best wavelet functions for constructing the approximate A4 wavelet are db4, bior2.4, bior2.6 and bior3.3 wavelet functions. Therefore, it can be concluded that the results obtained for making approximate waves in multi-degree-of-freedom structures are also very close to single-degree-of-freedom systems. Therefore, it can be said that to choose the best wavelet function for different earthquakes, one can use the analysis of single degree of freedom systems. In the Table (4), the results for different CDFs are presented. In fact, from the results obtained from the structural analysis of several degrees of freedom used in this article, it is possible to choose the appropriate wavelet function according to the required accuracy. In the Table (4), the CDF value for 5, 10, 15 and 20 percent errors is presented. In fact, the Table (4) shows the reliability of each approximate wavelet

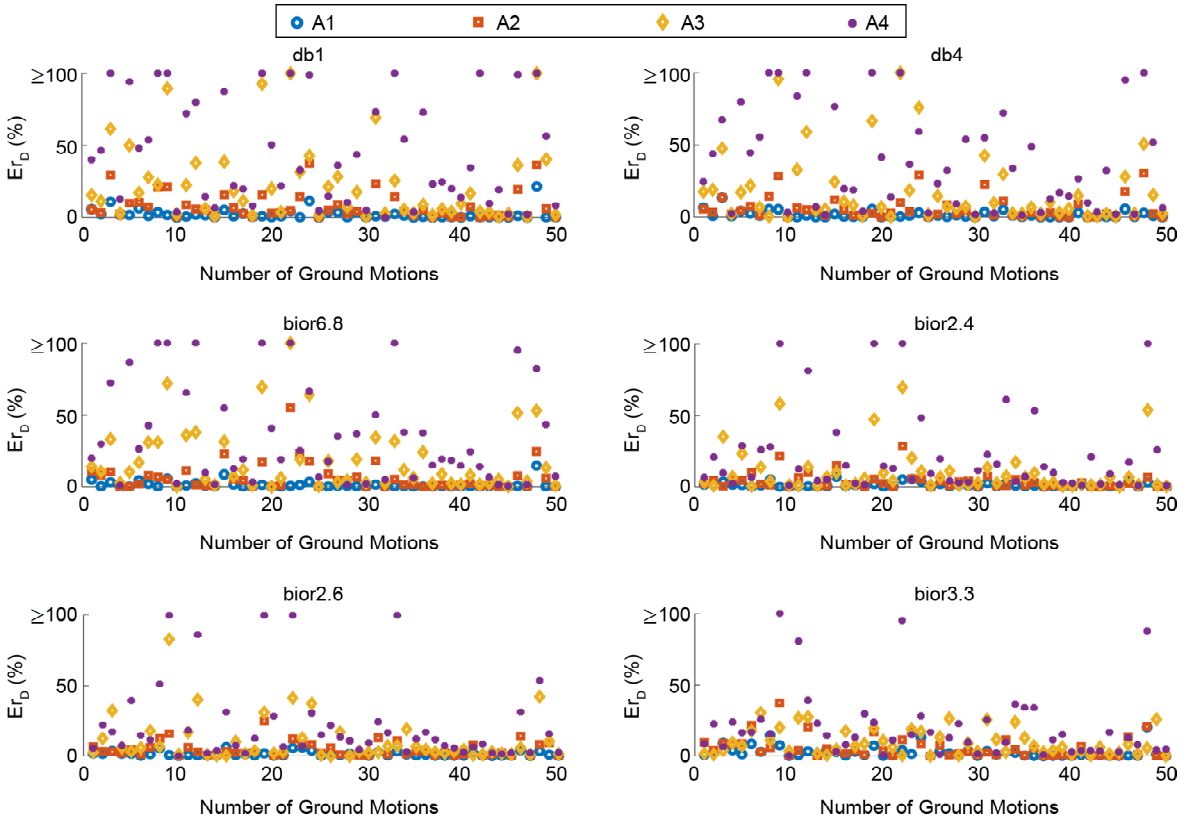

Figure 21. Roof displacement error.

for each wavelet function. For example, the CDF value of the approximate A3 wave for the db1 wavelet function is 34% if the error is less than 5%. This means that in only 34% of earthquakes, the calculation error for this approximate wave and this wavelet function was less than 5%.

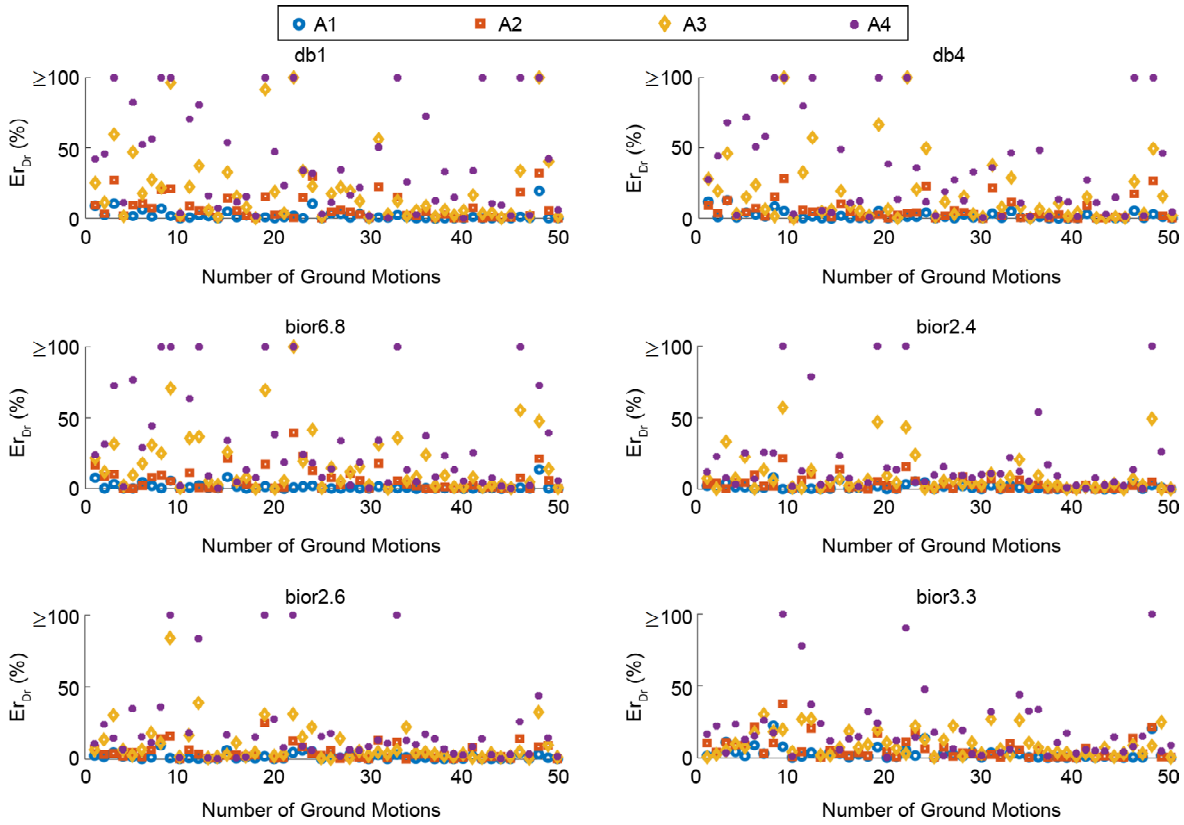

Figure 22. Drift error.

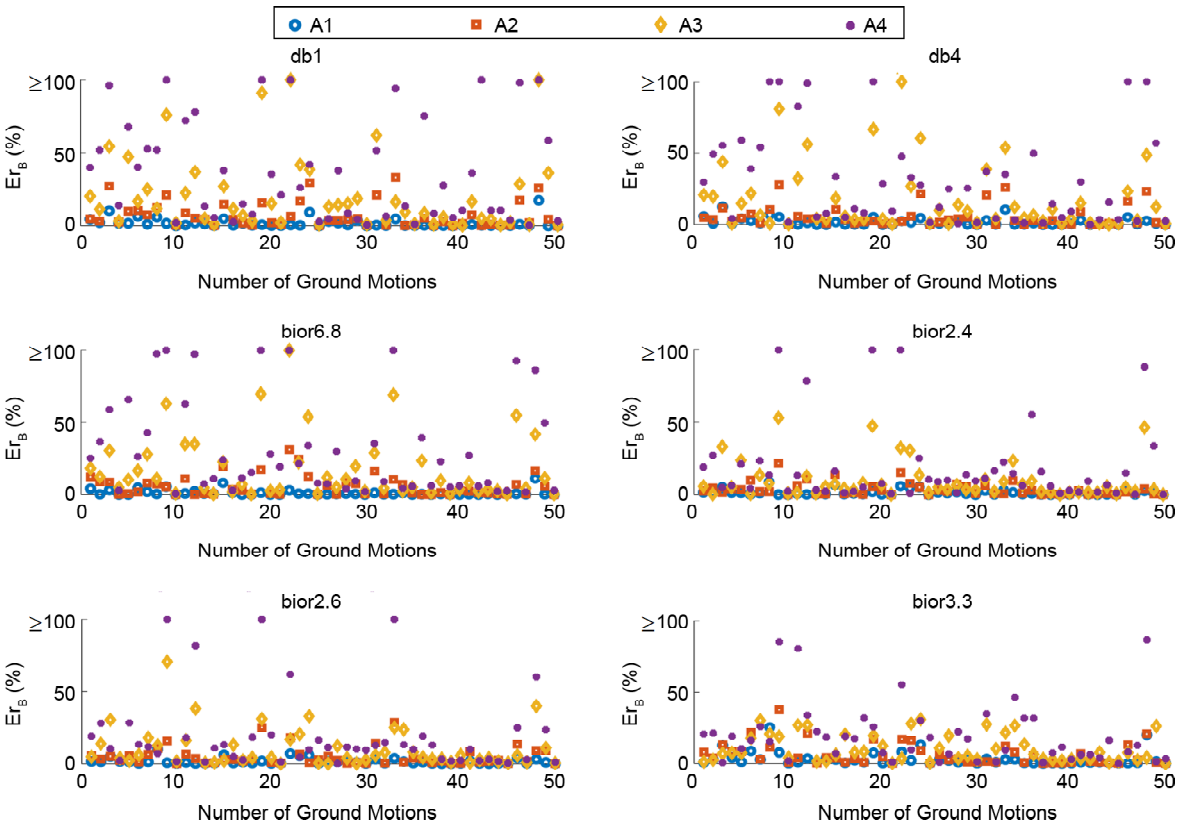

Figure 23. Base shear error.

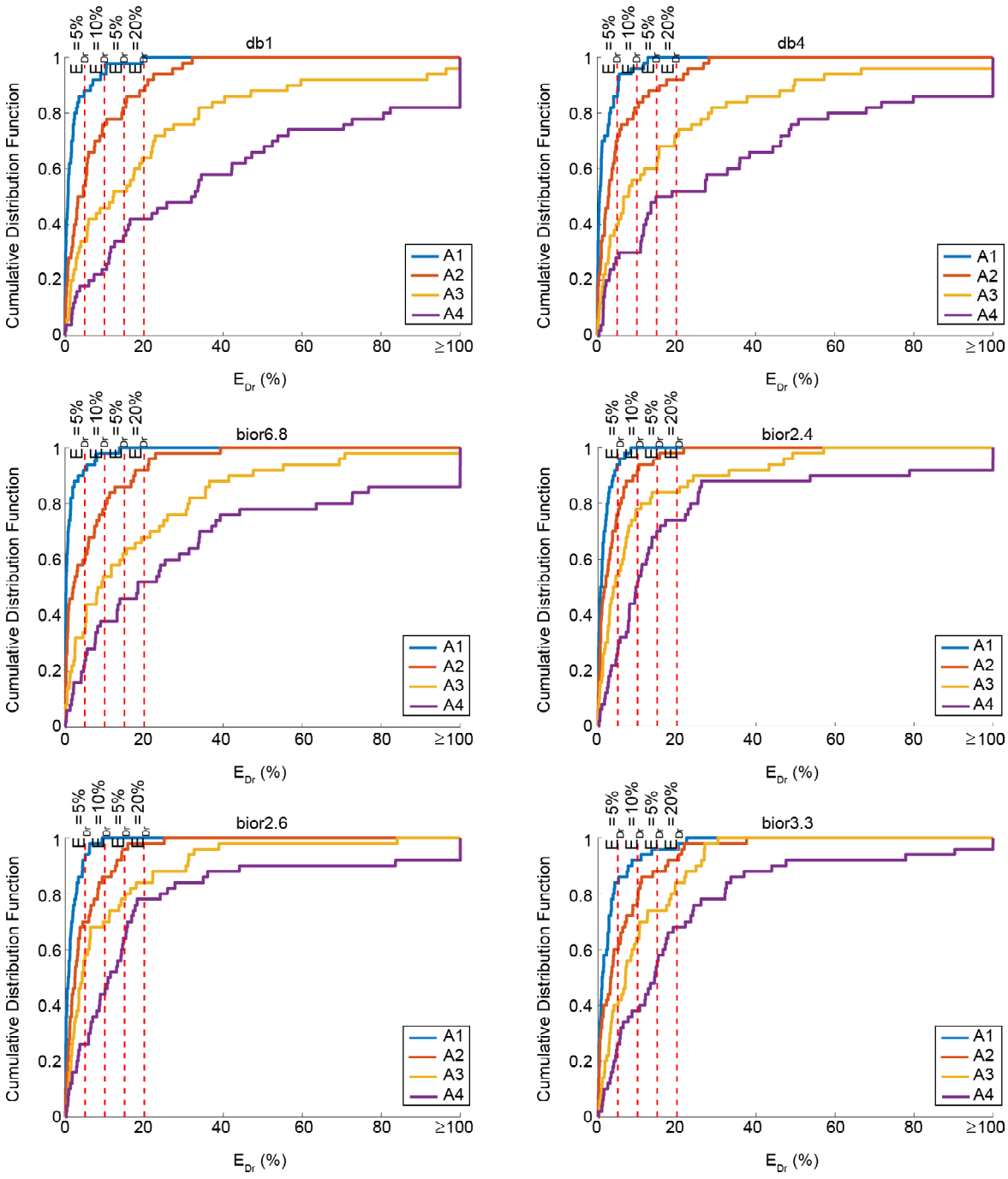

Figure 24. CDF curves for different wavelet functions.

Meanwhile, this value for the bior2.6 wavelet function was about 56%. This means that if the bior2.6 wavelet function is used, the error of the approximate A3 wave calculations was less than 5% in 56% of the earthquakes.

As mentioned, the purpose of reducing the sampling of earthquake waves is to increase the time step of the earthquake and, as a result, to increase the time step of the solution. Therefore, by increasing the time step of the solution, it is possible to reduce the cost of calculations and increase the speed of calculations. To show this, the figure below shows the analysis time of a 20-story structure for 50 earthquakes. As shown in the Figure (25), if the main earthquake is used to analyze the structure, the analysis time will take about 330 minutes. This is despite the fact that if the approximate waves A3 and A4 are used instead of the main earthquake, the analysis time will be about 50 minutes and 30 minutes. This means that using the approximate A4 wave can reduce the calculation cost by more than 90%.

Table 4. CDF for different wavelet functions and different approximate wavelets.

	Wave	E_{Dr}=5%	E_{Dr}=20%	E_{Dr}=15%	E_{Dr}=10%
CDF(%) for db1	A1	88	94	98	100
	A2	54	76	82	88
	A3	34	46	52	64
	A4	18	24	36	42
CDF(%) for db4	A1	86	96	100	100
	A2	70	82	88	92
	A3	40	56	60	72
	A4	28	30	50	52
CDF(%) for bior6.8	A1	92	98	100	100
	A2	60	78	86	92
	A3	34	54	62	68
	A4	24	38	46	52
CDF(%) for bior2.4	A1	94	100	100	100
	A2	76	92	96	98
	A3	54	78	84	84
	A4	28	52	70	74
CDF(%) for bior2.6	A1	92	100	100	100
	A2	70	86	96	98
	A3	56	70	78	84
	A4	26	44	64	78
CDF(%) for bior3.3	A1	84	92	96	96
	A2	60	78	88	92
	A3	40	64	74	84
	A4	26	38	54	68

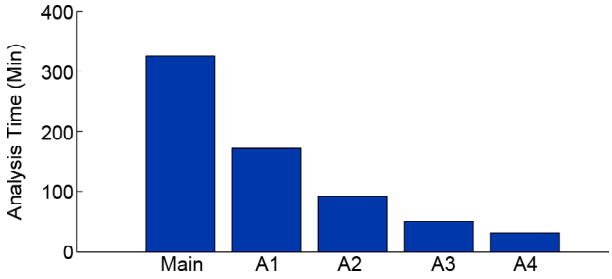

Figure 25. The cost of calculations for the analysis of 20-story structures.

7. Future Research Plan

In this article, it was shown that the use of wavelet-based down-sampling methods can significantly reduce the cost of calculations. As a perspective for the future, this topic can be developed in the following areas:

1. Examining the proposed method for nonlinear dynamic analysis of concrete structures
2. Combining wavelet-based down-sampling methods with other methods
3. Evaluation of wavelet-based down-sampling methods in regular and irregular three-dimensional structures

8. Conclusion

In this paper, for the first time, the simultaneous effect of wavelet function and numerical solution of vibration equations on the accuracy of wavelet-based dynamic analysis calculations was investigated. For this purpose, first, 50 earthquake records and 24 wavelet functions were selected. Then, single degree of freedom systems with a period of 0.05 to 10 seconds were investigated. In the next part, the effect of wavelet functions on the calculation accuracy of a 20-story frame was investigated. Based on the analysis, the following results were obtained.

- Based on the results obtained from different wavelet functions, it can be seen that the decomposition at level 5 (A5) with an error of more than 80% is not suitable for dynamic analysis.
- The Daubechies family wavelet functions, used in previous studies, are only suitable for the first (A1) and the second (A2) levels of decomposition. The error of the appropriate wavelet function of this wavelet family for these decomposition levels is often less than 5%.
- Using the appropriate wavelet transform can reduce the calculation error up to 10 times. For example, the average error of the approximate wave response spectrum A3 for the db1 wavelet function is about 20% and for the bior2.6 wavelet function is about 2%.

- Based on the results obtained from the analysis of the 20-story structure, Figure (19) confirms that the analysis using the approximate wave A4 derived from certain wavelet functions like db1, db4, bior6.8, bior2.4, and bior2.6 often diverges and yields high drift values. Conversely, A4 from bior2.4 and bior2.6 provides accurate results. Figure (20) reveals that A3 and A4 from db1, db4, and bior6.8 lack accuracy, while A1 to A3 from bior2.4 and bior2.6 demonstrate good accuracy. Notably, all approximate waves from bior3.3 exhibit good accuracy in both mean and median drift, as depicted in Figures (19) and (20).
- The analysis of a 20-story structure indicates that wavelet functions db1 and db4 are suitable solely for generating approximate waves A1 and A2. Statistical assessment reveals bior6.8, bior2.4, and bior2.6 as optimal for constructing A1 with a 5% maximum error. Bior2.4 is best for A2, bior2.6 for A3, and db4, bior2.4, bior2.6, and bior3.3 for A4. This suggests that results for approximate waves in multi-degree-of-freedom structures closely align with single-degree-of-freedom systems. Thus, single-degree-of-freedom system analyses can guide the selection of wavelet functions for various earthquakes. The presented CDF illustrates the reliability of each approximate wavelet for different wavelet functions, such as 34% for db1 and 56% for bior2.6, indicating the frequency of earthquakes where calculation errors are less than 5%.
- In the analysis of the 20-story structure, it was shown that the cost of calculations can be reduced by 90% using wavelet transform with an acceptable error.
- For the application of this method in engineering problems in order to analysis various structures, if the maximum error of 10% is accepted as an acceptable error, it is suggested to use two level of decomposition of the approximate waves obtained by the wavelet method. In this case, the cost of calculations can be reduced by more than 70%.

References

Alonso, R. J., Noori, M., Saadat, S., Masuda, A., & Hou, Z. (2004). Effects of excitation frequency on detection accuracy of orthogonal wavelet decomposition for structural health monitoring. *Earthquake Engineering and Engineering Vibration*, *3*(1), 101-106.

Bitaraf, M., Hurlebaus, S., & Barroso, L.R. (2012). Active and semi-active adaptive control for undamaged and damaged building structures under seismic load. *Computer-Aided Civil and Infrastructure Engineering*, *27*(1), 48-64. https://doi.org/10.1111/j.1467-8667.2011.00719.x

Chopra, A.K. (2012). Dynamics of Structures, 4th. New Jersey: Prentice Hall. [Record #40 is using a reference type undefined in this output style.]

Council, B.S.S. (2000). *Prestandard and Commentary for the Seismic Rehabilitation of Buildings*. Report FEMA-356, Washington, DC.

Dadkhah, M., Kamgar, R., & Heidarzadeh, H. (2020). Reducing the cost of calculations for incremental dynamic analysis of building structures using the discrete wavelet transform. *Journal of Earthquake Engineering*, 1-26. https://doi.org/10.1080/13632469. 2020.1798830

Daubechies, I. (1992). *Ten Lectures on Wavelets*. SIAM.

Ghaffary, A., & Moustafa, M.A. (2021). Performance-based assessment and structural response of 20-story SAC building under wind hazards through collapse. *Journal of Structural Engineering*, *147*(3), 04020346.

Gupta, A., & Krawinkler, H. (1998). *Seismic Demands for the Performance Evaluation of Steel Moment Resisting Frame Structures*. Stanford University.

Heidari, A., & Majidi, N. (2021). Earthquake acceleration analysis using wavelet method. *Earthquake Engineering and Engineering Vibration*, *20*(1), 113-126. https://doi.org/10.1007/s11803-021-2009-8

Heidari, A., Pahlavan sadegh, S., & Raeisi, J. (2019). Investigating the effect of soil type on non-linear response spectrum using wavelet theory. *International Journal of Civil Engineering*,

17(12), 1909-1918. https://doi.org/10.1007/s40999-019-00394-6

Hémon, P., & Santi, F. (2007). Simulation of a spatially correlated turbulent velocity field using biorthogonal decomposition. *Journal of Wind Engineering and Industrial Aerodynamics*, *95*(1), 21-29. https://doi.org/10.1016/j.jweia.2006.04.003

Hilber, H.M. (1976). *Analysis and Design of Numerical Integration Methods in Structural Dynamics*. University of California, Berkeley.

Hossain, M.R., Ashraf, M., & Padgett, J.E. (2013). Risk-based seismic performance assessment of yielding shear panel device. *Engineering Structures*, *56*, 1570-1579. https://doi.org/10.1016/j.engstruct.2013.07.032

Hosseini, M., Moghaddam, S.A., & Emami, S.M.M. (2013). A method for simplification of earthquake accelerograms for rapid time history analysis based on time-frequency representations conference. *Proceedings of the 11th International Conference on Vibration Problems (ICoVP)*.

Javdanian, H., Heidari, A., & Raeisi, J. (2021). Seismic ground response under wavelet-based decomposed earthquake records. *Soil Dyn. Earthq. Eng.*, *149*, 106865. https://doi.org/10.1016/j.soildyn.2021.106865

Jena, S.K., Chakraverty, S., & Malikan, M. (2021). Implementation of haar wavelet, higher order Haar wavelet, and differential quadrature methods on buckling response of strain gradient nonlocal beam embedded in an elastic medium. *Engineering with Computers*, *37*(2), 1251-1264. https://doi.org/10.1007/s00366-019-00883-1

Jia, L.-J., Xiang, P., Wu, M., & Nishitani, A. (2018). Swing story-lateral force resisting system connected with dampers: Novel seismic vibration control system for building structures. *Journal of Engineering Mechanics*, *144*(2), 04017159.

Kamgar, R., Dadkhah, M., & Naderpour, H. (2021). Seismic response evaluation of structures using discrete wavelet transform through linear analysis. *Structures*, *29*, 863-882. https://doi.org/10.1016/j.istruc.2020.11.012

Kamgar, R., Dadkhah, M., & Naderpour, H. (2022). Earthquake-induced nonlinear dynamic response assessment of structures in terms of discrete wavelet transform. *Structures*, *39*, 821-847. https://doi.org/10.1016/j.istruc.2022.03.060

Kamgar, R., Majidi, N., & Heidari, A. (2020). *Wavelet-Based Decomposition of Ground Acceleration for Efficient Calculation of Seismic Response in Elastoplastic Structures*. Periodica Polytechnica Civil Engineering. https://doi.org/10.3311/PPci.14475

Kamgar, R., Tavakoli, R., Rahgozar, P., & Jankowski, R. (2021). Application of discrete wavelet transform in seismic nonlinear analysis of soil-structure interaction problems. *Earthquake Spectra*. https://doi.org/10.1177/8755293020988027

Kankanamge, Y., Hu, Y., & Shao, X. (2020). Application of wavelet transform in structural health monitoring. *Earthquake Engineering and Engineering Vibration*, *19*(2), 515-532.

Majidi, N., Heidari, A., Alireza, F., & Heidarzadeh, H. (2022). Estimation of earthquake frequency content and its effect on dynamic analysis using continuous and discrete wavelet transform. *Scientia Iranica*. https://doi.org/10.24200/SCI.2022.54226.3662

Majidi, N., Riahi, H.T., & Zandi, S.M. (2023). Evaluating the performance of different mother wavelet functions for down-sampling of earthquake records. *Structures*, *51*, 846-879.

Majidi, N., Riahi, H.T., Zandi, S.M., & Hajirasouliha, I. (2023). Development of practical downsampling methods for nonlinear time history analysis of complex structures. *Soil Dynamics and Earthquake Engineering*, *175*, 108247.

Majidi, N., Tajmir Riahi, H., & Zandi, M. (2022). Reducing computational efforts in linear and nonlinear analysis of peridynamic models under impact loads. *Amirkabir Journal of Civil & Environmental Engineering*. https://doi.org/10.22060/CEEJ.2022.20075.7337

Mallat, S. (1999). *A Wavelet Tour of Signal Processing*. Elsevier.

Mazzoni, S., McKenna, F., Scott, M.H., & Fenves, G.L. (2006). *Open System for Earthquake Engineering Simulation User Command-Language Manual*. Report NEES grid-TR 2004, 21.

Mehr Motlagh, M., Bahar, A., & Bahar, O. (2021). Investigation of soil-structure interaction effects on damage detection of wind turbine tower with biorthogonal wavelets. *Amirkabir Journal of Civil Engineering*, *53*(6), 19-19. https://doi.org/10.22060/CEEJ.2021.17394.6566

Misiti, M., Misiti, Y., Oppenheim, G., & Poggi, J.-M. (1996). *Wavelet Toolbox User's Guide*. The Math Works Inc.

Nagarajaiah, S., & Basu, B. (2009). Output only modal identification and structural damage detection using time frequency & wavelet techniques. *Earthquake Engineering and Engineering Vibration*, *8*(4), 583-605.

Nasab, M.S.E., & Kim, J. (2020). Seismic retrofit of structures using hybrid steel slit-viscoelastic dampers. *Journal of Structural Engineering*, *146*(11), 04020238.

Nateghi, F. (2011). On Less Computational Costs for Analysis of Silos Seismic Behavior by Time Integration Computational Methods in Structural Dynamics and Earthquake Engineering, ???.

Nigam, N.C., & Jennings, P. C. (1968). *Digital Calculation of Response Spectra from Strong-Motion Earthquake Records*. California Institute of Technology, Earthquake Engineering Research ….

Nigam, N.C., & Jennings, P.C. (1969). Calculation of response spectra from strong-motion earthquake records. *Bulletin of the Seismological Society of America*, *59*(2), 909-922.

Pandit, S., & Sharma, S. (2020). Wavelet strategy for flow and heat transfer in CNT-water based fluid with asymmetric variable rectangular porous channel. *Engineering with Computers*, 1-11. https://doi.org/10.1007/s00366-020-01139-z

Pnevmatikos, N.G., & Hatzigeorgiou, G.D. (2017). Damage detection of framed structures subjected to earthquake excitation using discrete wavelet analysis. *Bulletin of Earthquake Engineering*, *15*(1), 227-248.

Qiu, C., Zhao, X., & Zhu, S. (2020). Seismic upgrading of multistory steel moment-resisting frames by installing shape memory alloy braces: design method and performance evaluation. *Structural Control and Health Monitoring*, *27*(9). https://doi.org/10.1002/stc.2596

Salajegheh, E., & Heidari, A. (2002). Dynamic analysis of structures against earthquake by combined wavelet transform and fast Fourier transform. *Asian Journal of Civil Engineering*.

Salajegheh, E., & Heidari, A. (2004). Optimum design of structures against earthquake by adaptive genetic algorithm using wavelet networks. *Structural and Multidisciplinary Optimization*, *28*(4), 277-285. https://doi.org/10.1007/s00158-004-0422-z

Salajegheh, E., & Heidari, A. (2005). Optimum design of structures against earthquake by wavelet neural network and filter banks. *Earthquake Engineering & Structural Dynamics*, *34*(1), 67-82. https://doi.org/10.1002/eqe.417

Sepasdar, R., Banan, M.R., & Banan, M.R. (2019). A numerical investigation on the effect of panel zones on cyclic lateral capacity of steel moment frames. *Iranian Journal of Science and Technology, Transactions of Civil Engineering*, 1-10. https://doi.org/10.1007/s40996-019-00274-y

Shayanfar, M., Rakhshanimehr, M., & Bidoki, R.Z. (2016). An energy based adaptive pushover analysis for nonlinear static procedures. *Civil Engineering Infrastructures Journal*, *49*(2), 289-310. https://doi.org/10.7508/CEIJ.2016.02.007

Soroushian, A. (2008). A technique for time integration analysis with steps larger than the excitation steps. *Communications in Numerical Methods in Engineering*, *24*(12), 2087-2111.

Soroushian, A., Saaed, A., Arghavani, M., Rajabi, M., & Sharifpour, M. (2011). Less computational costs in the analysis of reservoirs seismic behaviors by time integration. *Vibration Problems ICOVP 2011: the 10th International Conference on Vib-ration Problems*.

Spanos, P., & Rao, V.R.S. (2001). Random field representation in a biorthogonal wavelet basis. *Journal of Engineering Mechanics*, *127*(2), 194-205. https://doi.org/10.1061/(ASCE)0733-9399(2001)127:2(194)

Teng, Y.-T., Wang, X.-Z., Wang, X.-M., Ma, J.-M., & Xu, J.-H. (2006). P wave onset time picking with the B-spline biorthogonal wavelet. *Acta Seismological Sinica*, *19*(3), 350-355. https://doi. org/ 10.1007/s11589-003-0350-9

Venture, S.J. (2000). *State of the Art Report on Systems Performance of Steel Moment Frames Subject to Earthquake Ground Shakin*g. FEMA 355C.

Wang, X., Teng, Y., Qu, B., & Zhang, M. (2011). Seismic data lossy compression and distortion analysis. J*ournal of Earthquake Engineering and Engineering Vibration*, *4*.